University of Stavanger

Faculty of Science and Technology

MASTER'S THESIS

Study program/ Specialization: Petroleum technology - Drilling	Spring semester, 2012 Open / Restricted access
Writer: Henning Stave	…… (Writer's signature)
Faculty supervisor: Gerhard Nygaard Co-supervisor: Espen Hauge	
Title of thesis: Evaluation of kick and loss scenarios in experimental lab facility	
Credits (ECTS): 30	
Key words: Detection and evaluation of kick and loss Small scale rig	Pages: 50 + enclosure: 34 Stavanger, June 14, 2012 Date/year

Henning Stave

Master's thesis

Evaluation of kick and loss scenarios in experimental lab facility

University of Stavanger, Spring 2012

Preface

This master thesis presents an evaluation of kick and loss scenarios in experimental lab facility located at UiS. The work presented in this paper is largely based on the work presented in the master thesis of Alexander Wang and Magnus Tveit Torsvik who built the rig and wrote the control algorithms.

The background for this thesis is the desire for a higher degree of automation of drilling. Kick and loss situations are today manually evaluated by the drilling crew. Sufficient training and experience is crucial to make quick and correct decisions when dealing with situations that can evolve to become critical or result in unnecessary NPT. Still, manual evaluation leaves room for human error.

As a part of the automation of drilling process, typical responses of the wellbore fluid dynamics need to be identified. This paper presents a series of experiments that show how different influx- and loss scenarios affect the flow- and pressure responses in the system.

I would like to thank:

My supervisor Gerhard Nygaard, for his suggestions to experimental tests, and for giving me a crash course in Matlab.

Co-supervisor Espen Hauge, for providing feedback on the tests.

Former student Alexander Wang, for making time to show me the basics on how to run the rig and operate it from the Simulink model.

Abstract

Detection and evaluation of gain and loss situations is crucial for safety during drilling operations. During managed pressure drilling there is higher risk of kicks than during traditional drilling. Early stage detection and evaluation are of importance in order to avoid situations that can evolve into critical incidents.

The main focus in the project will be to detect and evaluate kick and loss during drilling operations, primarily based on experiments performed on small scale lab. facility. Experiments will be performed with the intention to investigate how different influx- and loss scenarios will affect the flow- and pressure responses in the system. Pressure transmitters installed in the system are used in comparison to pumprate and Coriolis flowrate.

The results from the experiments are used to correlate the different pressure readings to each other, and to determine the relation between flow- and pressure responses for different scenarios. The results show that pressure transmitters measure a larger relative change in pressure compared to the relative change in flowrate obtained from Coriolis data. This indicates that monitoring pressure changes in the system can be an effective way to detect gain- or loss situations.

Table of Contents

Faculty of Science and Technology

MASTER'S THESIS

Nomenclature

AFP	Annular Friction Pressure
BHP	Bottom Hole Pressure
BOP	Blow Out Preventer
BPP	Back Pressure Pump
DG	Dual Gradient
FP	Fracture Pressure
HH	Hydrostatic Head
HSE	Health, Safety and Environment
LCM	Lost Circulation Materials
MPD	Managed Pressure Drilling
MWD	Measurements While Drilling
NPT	Non Productive Time
P&ID	Piping and Instrumentation Diagram
PP	Pore Pressure
PT	Pressure Transmitter
RCD	Rotating Control Device
ROP	Rate Of Penetration

1. Introduction

1.1. Small scale laboratory facility

The main focus in the project will be to detect and evaluate kick and loss during drilling operations, primarily based on experiments performed on small scale lab. facility.

Experiments will be performed with the intention to investigate how different influx- and loss scenarios will affect the flow- and pressure responses in the system. Pressure transmitters located in standpipe, downhole, top of annulus before MPD choke and at surface will be used in comparison to pumprate and Coriolis flowrate.

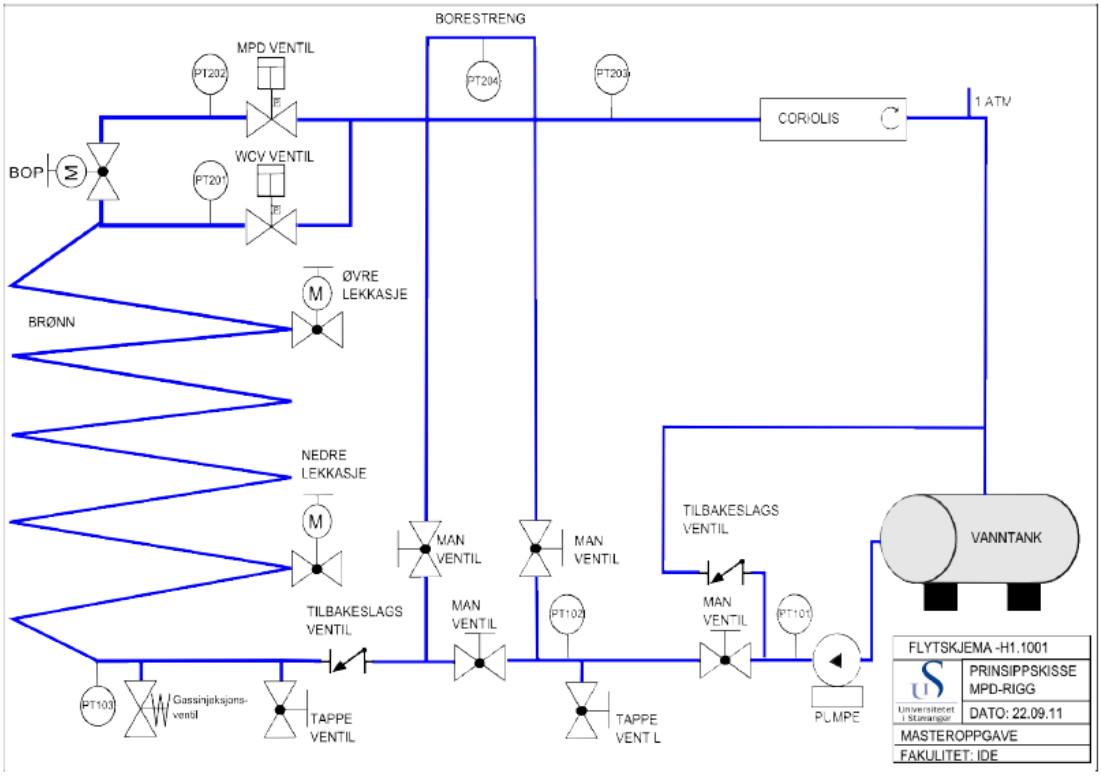

Figure 1.1: P&ID of small scale rig located at UiS. Figure taken from A.Wang [1].

1.2. Managed-Pressure Drilling

Managed-pressure drilling (MPD) is an advanced form of primary well control that usually has a closed and pressurizable mud system. This is needed to be able to operate with BHP very close to the PP. Formation fluid influx into the well is not wanted with MPD, but one is equipped to handle it safely if it occurs incidentally.

Most of the world's easy targets have already been drilled. One of the properties of an easy target is a wide drilling window (large difference between PP and FP). During traditional drilling a wide drilling window is needed to avoid kick or loss, especially in high temperature, high pressure wells. In the smaller sized hole-sections the annular friction pressure (AFP) is a considerable part of the BHP. Making connections with a conventional open to atmosphere mud-return system will cause the BHP to decrease with a value equivalent to the AFP. If the HH alone is less than the PP, we have a kick situation. Equivalent to this is the situation where the sum of HH and AFP exceeds the FP and mud is lost into the formation.

We distinguish between reactive and proactive MPD. Both require the rig to have much of the same equipment installed, at least an RCD, choke, and drillstring floats. As the name tells us, reactive MPD is used as a contingency in case of downhole surprises. The proactive MPD program is designed to precisely manage the wellbore pressure profile. [2]

MPD is not restricted to narrow pressure margin drilling, new technology have opened up for other applications. Until recently, MPD could be divided into four classifications: Constant Bottomhole Pressure (CBHP), Dual Gradient Drilling (DGD), Pressurized Mudcap Drilling (PMCD) and Zero Discharge or Health Safety and Environmental (HSE) [3].

Lowering of the dynamic overbalance pressure has significant advantages even where the pressure margin is large enough for traditional drilling. Reduction in differential pressure at the bit-rock interface means that the cuttings can be removed more easily which typically results in a higher ROP. Another major advantage with MPD is enhanced kick and loss detection. MPD uses additional equipment like Coriolis and Micro-Flux flowmeters to achieve better control of the wellbore pressure profile by monitoring variations in the fluid flow. [3]

2. Influx and loss during drilling operations

2.1. Well control system

The well control system is functioning as, like the name suggests, a system to control the well. It permits detection of kicks, well shut-in by closing the BOP, circulating the kick out through a designated chokeline and divert the flow safely away from rig personnel and equipment. [4] The well control system is essential for the safety on the rig during drilling operations.

2.2. Overview of the various causes for influx and losses

2.2.1. Causes for influx

A kick is unwanted influx of formation fluid into the wellbore. This will happen when the pressure in the formation, called pore pressure, exceeds the borehole pressure.

Illustration by example: While drilling a conventional overbalanced well, a gas kick is taken in the well when connecting a new stand of drillpipe to the string. While circulating, the bottomhole pressure is the sum of the hydrostatic pressure of the mud column plus the dynamic pressure loss caused by annular friction. When a connection is to be made, mud pumps are stopped, and the bottomhole pressure falls to hydrostatic pressure. In this case, the hydrostatic pressure alone is not enough to exceed the pore pressure, and a kick is taken. The fluid influx is consisting of gas, which presents a potentially dangerous situation. The formation fluid density is lower than that of the drilling fluid, so the hydrostatic pressure is lowered when the mud is diluted or replaced (cut) with gas, and if the situation is not detected and controlled this will lead to a blow-out.

During conventional drilling, great effort is made to keep the borehole pressure between the pore pressure and the fracture pressure. If a kick is taken, the standard way to obtain well

control is to “kill” the well. To kill the well basically means to create a hydrostatic pressure that is sufficient to overcome the formation pressure and hence stop formation fluid from entering the well.

There is some uncertainty in pore pressure, especially while exploring new formations. Wrong mud weight might lead to a kick- or loss situation. If the pressure created by the mudweight is insufficient to repress the formation pressure from forcing fluids into the well, a kick will be the result. This is one of the predominant reasons for kicks [5]. Insufficient refill of the well while tripping out of the hole is another frequently encountered cause of kicks [5]. The annular mud level will sink when pipe is removed, and as a result the bottomhole pressure will decrease. Yet another important consideration is swab effects caused by tripping or heave, which might lead to kick when the margin between pore pressure and hydrostatic pressure is low.

2.2.2. Causes of loss

Loss situations happen for instance when the borehole pressure exceeds the fracture pressure of the formation. Cracks are then created, and mud is lost to the formation. There are several reasons to avoid mud loss. First of all, some drilling fluids are very expensive, so flushing it into the formation is poor economics. Equally important is the formation skin damage that could occur if a producing zone is fractured. Loss situations also occur frequently when formations with very high permabilities are entered, or when drilling into a cave system. For all of these cases, high mudlosses constitutes a risk with respect to well control. If the mudloss rate is higher than the pump rate, the mud column will sink, and hydrostatic pressure will decrease which again could lead to a kick.

3. Detection procedures for influx and loss

3.1. Manual procedures

3.1.1. Monitored parameters

A kick can be detected by mud pit level increase while drilling, or by higher flow rate measurements out of the well than into the well. Another possible way to detect kicks is by observing the derrick hookload. Since the formation fluids that enter the well during a kick almost always are less dense than the drilling fluid, the effective weight of the drillstring will increase due to the reduced buoyancy. Also, if the well keeps flowing after the pumps have been turned off, this can be an indicator of kick. However, this might not be the case. Deep, high-temperature wells will cause the mud to expand and can cause the well to flow after circulation has been stopped. It is therefore important to differentiate between the behaviour of flow-back caused by temperature effects and by kicks. The way this is done is by a method called fingerprinting, but this will not be discussed in detail in this paper.

Flow measurements at the inlet and outlet of the well, and the discrepancy between these rates are used as an indicator of kick- and loss situations. There are however certain phenomena that will affect the rate out of the well without having influx from or loss to the nearby formation. Temperature effects will typically expand the drilling fluid, so a higher outflow rate is expected due to reduced density of the mud. While drilling the well, the mud will always be ”diluted” with rock and formation fluids. Of course, the drilled formation and formation fluids also add to the total outflow. A drilling fluid that have a lower density when it comes out of the well than when it went in due to presence of gas bubbles, is said to be gas cut [4]. A remarkable reduction in density and volume flow out of the well can be achieved, even if there is no influx into the well from the surrounding formation. This scenario can occur even in tight formations, and should not be confused with a kick.

Example 3.1.

■

Illustration by a simplified example assuming ideal gas behaviour and that both gas and cuttings have the same annular velocity as the mud, also neglecting friction, filtrate loss and temperature effects. This example will produce exaggerated results, as we also assume that all gas will be released from the cuttings. This scenario is for a conventional well were annular mudflow returns to atmospheric pressure.

Drilling with an ROP of 15 m/hr with an 8,5 inch bit through low permeability sandstone containing methane gas at 4000 m. TVD. Formation and well properties are shown in the table below.

Parameters				
Permeabiliy	0	[mD]	0	[mD]
Porosity	0,3		0,3	
Water saturation	0,25		0,25	
	0,75		0,75	
Rate of penetration	15	[m/hr]	0,004167	[m/s]
Depth	4000	[m]	4000	[m]
Mud weight	1,7	s.g.	1,7	s.g.
Average mud temperature	70	[C]	70	[C]
Formation water density	1,1	s.g.	1,1	s.g.
Drilled solids density	2,6	s.g.	2,6	s.g.
Circulation rate	1350	[l/min]	0,0225	[m^3/s]
Drill bit size	8,5	[in]	0,2159	[m]

Table 3.1: Well and formation parameters

Hydrostatic pressure :

$$P = \rho * g * h = MW * 0,0981 * TVD = 1,70 * 0,0981 * 4000 = 667,08 \text{ bar}$$

$$\text{Added formation and formation fluids} = ROP * A_{hole}$$

$$0,004167 * 0,2159 \wedge 2 * \pi / 4 = 0,000153[m^3/s] = 9,152404[l/min]$$

This corresponds to a 0,68 % relative increase in outflow if formation containing incompressible fluid is drilled. When drilling through formation containing gas the situation becomes quite different.

Drilled solids are being added to the drilling fluid at the rate of:

$$9,152404[l/\min]*(1-0,3)=6,4067[l/\min]$$

Formation water is being added to the drilling fluid at a rate of:

$$9,152404[l/\min]*0,3*0,25=0,68643[l/\min]$$

Methane gas is being added to the drilling fluid at a rate of:

$$9,152404[l/\min]*0,3*0,75=2,059291[l/\min]$$

For simplicity we consider methane to be an ideal gas with molecular mass 16,042 [g/mol]

$$\text{Using the equation of state: } P*V=n*R*T$$

$$\Rightarrow P*V=\frac{m}{M}*R*T \Rightarrow \frac{m}{V}=\frac{P*M}{R*T}=\rho$$

$$\rho=\frac{667*10^{5}*16,042*10^{-3}}{8,3144*(70+273,15)}=375,033[kg/m^{3}]=0,375\,\text{s.g.}$$

The mass rate of gas entering the well will then be:

$$\frac{\rho[\frac{kg}{m^{3}}]*q[\frac{m^{3}}{s}]}{M[\frac{g}{mol}]*10^{-3}}=\frac{375,033*2,059291*\frac{1}{1000}}{16,042*10^{-3}}=48,1425\left[\frac{mol}{\min}\right]$$

Which corresponds to 0,802375 moles pr. second.

Total flow up the annulus close to the bit will then become:

$$1350[\frac{l}{\min}]+9,152404[\frac{l}{\min}]=1359,152404[\frac{l}{\min}]$$

1 cubic meter of annular mud will then contain:

$$\frac{48,142503[\frac{mol}{min}]*1000[\frac{l}{m^3}]}{1359,1524040[\frac{l}{min}]}=35,420975[\frac{mol}{m^3}]$$

To find the relative increase in outflow, we will first find the gas cut mud density at surface:

At bottomhole 1 mole of gas will occupy:

$$\frac{n*R*T}{P}=\frac{1*8,3144*(70+273,15)}{667*10^5}=4,27749*10^{-5}$$

At atmospheric the volume will be (not accounting for change in temperature):

$$4,27749*10^{-5}*667=0,028530864[m^3]$$

This gives:

$$0,028530864[\frac{m^3}{mol}]*48,14250385[\frac{mol}{min}]=1,373547182[\frac{m^3}{min}]$$

in addition to the pumprate of 1,35 $[\frac{m^3}{min}]$

This gives the total flowrate out of the well:

$$1,373547182+1,35=2,723547182[\frac{l}{min}]$$

The mass of gas pr. litre of mud is:

$$0,016042[\frac{kg}{mol}]*0,035420975[\frac{mol}{l}]=0,000562[\frac{kg}{l}]$$

The gas cut mud density at surface will then be:

$$\frac{Q_{mud}*\rho_{mud}}{Q_{total}}+\frac{Q_{gas}*\rho_{gas}}{Q_{total}}=\frac{1,35[\frac{m^3}{min}]*1,7[s.g.]}{2,723547182[\frac{m^3}{min}]}+\frac{1,373547182[\frac{m^3}{min}]*0,000562[s.g.]}{2,723547182[\frac{m^3}{min}]}=0,842934519[s.g.]$$

Depth: Di denotes the depth for i meter, $i \in [0, 4000]$

$P_d i$: Hydrostatic pressure in drillpipe [bara] at depth Di,

$$P_d i = \rho_{mud} * Di * 0,0981 + 1$$

$V_{gas} i$: Volume occupied by 1 mole of gas [m^3] at depth Di,

$$V_{gas} i = \frac{1 * R * T}{Pi}$$

$\rho_{gas} i$: Density of methane at depth Di,

$$\rho_{gas} i = \frac{Pi * M_{gas}}{R * T}$$

$Q_{mixed} i$: Volume flow mixed fluid at depth Di,

$$Q_{mixed} i = Q_{i=4000\,total} * \left[(\text{fraction of incompressible mud}_{(\text{mud+rock+formation water})} \text{ at i=4000}) + \left(\frac{\frac{m_{gas}}{V_{mud}} * R * T}{Pi * M} \right) \right]$$

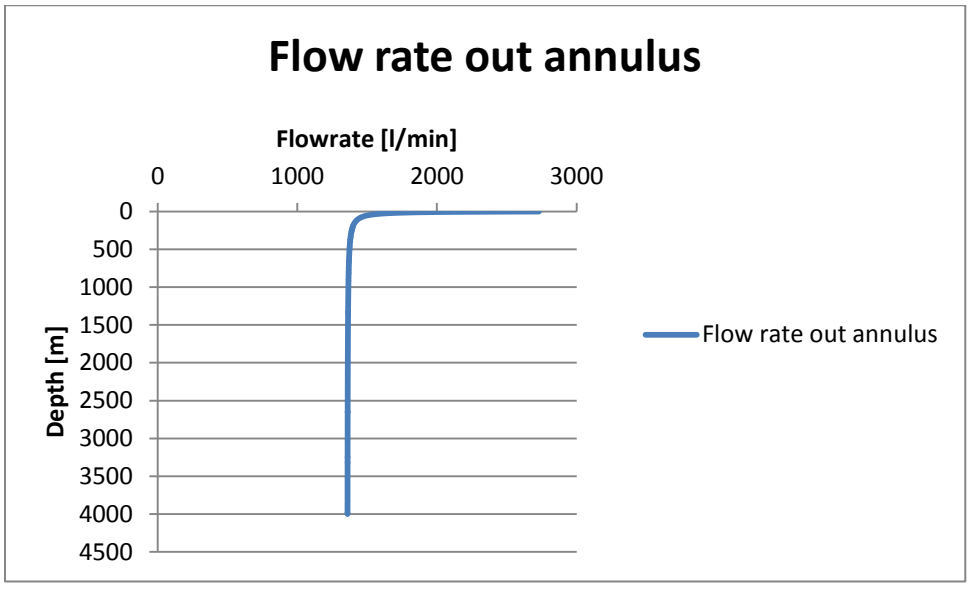

Figure 3.1.1: Volume flowrate through annulus as function of depth.

$Q_{gas}i$: Volume flow gas at depth Di,

$Q_{gas}i = Q_{mixed}i - Q_{MM}$

where the denotion $_{MM}$ stands for "mixed mud with rock and water excluding gas"

The gas expands violently in the upper part of the well.

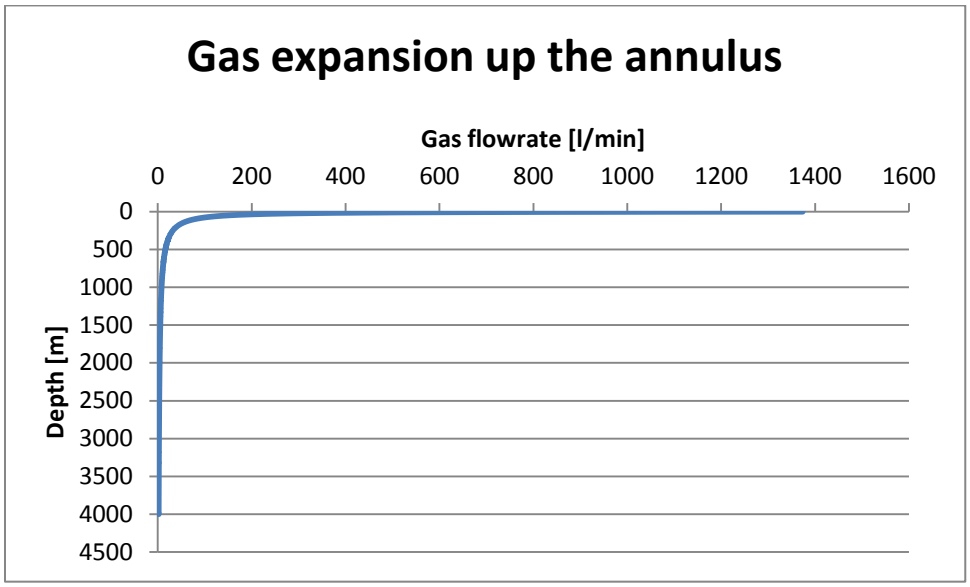

Figure 3.1.2: Gas volume flowrate through annulus as function of depth

This gas expansion results in a dramatically increased flowrate out of the hole, and reduction in density at surface.

$\rho_{mixed}i$: Density of mixed fluid at depth Di,

$$\rho_{mixed}i = \frac{Q_{MM}}{Q_{mixed}i} * \rho_{MM} + \frac{Q_{gas}i}{Q_{mixed}i} * \rho_{gas}i$$

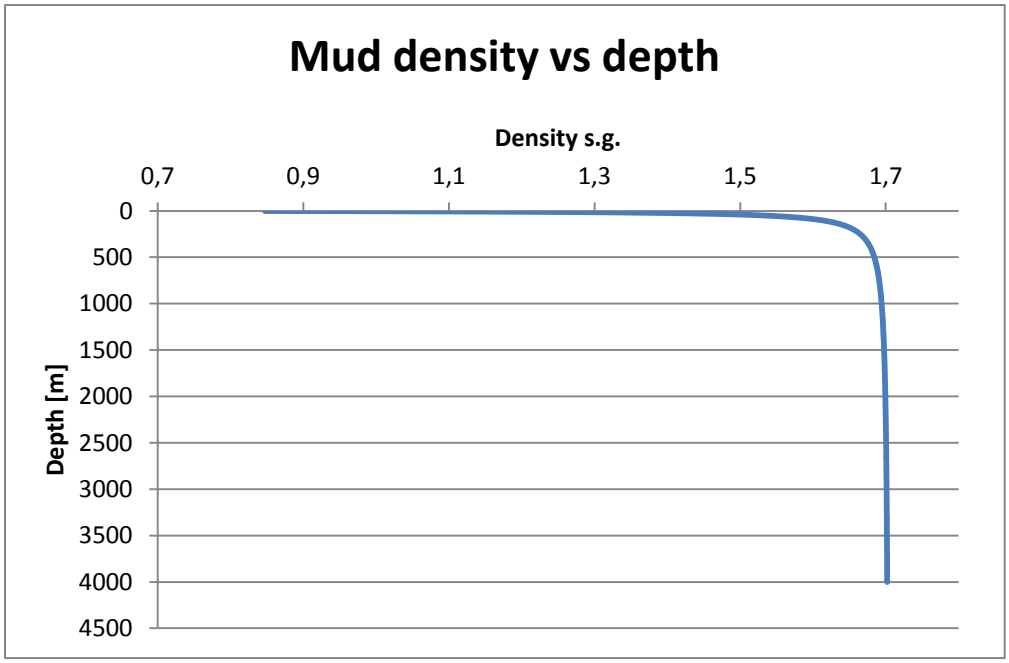

Figure 3.1.3: Mud density as function of depth

Since the density reduction primarily takes place in the uppermost part of the well, the total change in hydrostatic head for this scenario will not be very dramatic:

The hydrostatic pressure with gas in the well becomes:

$$P_a = \sum_{i=0}^{4000} 0,0981 * \rho_{mixed} i = 663,08 [bar]$$

We compare this with the hydrostatic pressure caused by undiluted mud:

ΔP = 667,08 [bar] – 663,08 [bar] = 4,0 [bar]

■

Example 3.1 shows that the flow measurements at the inlet and outlet of the well, and the discrepancy between these rates cannot always be used as a good indicator of kick. In the example the flowrate at the outlet is more than twice the pumprate. At a depth of 4000m the gas enters the well at a rate of 2 l/min, but at the outlet the rate is 1374 l/min. This is due to the violent gas expansion in the uppermost part of the open-to-atmosphere well.

The sum of simplifications done in this example contributes to a result that probably is larger than it would be without the simplifications. Still, the gas expansion can be found as some constant C multiplied with the product of a restricted gas volume and the pressure in this volume. In general Boyle's law give: $C * \frac{P_1 * V_1}{P_2} = V_2$,

for example 3.1: $1 * \frac{2,0593[l/\min] * 667,08[bar]}{1[bar]} = 1374[l/\min]$.

The graph in figure 3.1.2. illustrates an important difference between a real well versus the test rig. The hydrostatic pressure difference in the test rig is only 0,4 bar, and most of the gas expansion effect has therefore already taken place when the gas enter the annular flow.

3.2. Automatic procedures

3.2.1. Improvements and new technology

In order to detect and handle gain- or loss situations automatically, additional equipment is required. Coriolis flowmeters and Micro-Flux control meters are examples of tools that are utilized to enhance kick-loss detection. [3, 6, 7]

There has been done considerable improved on kick management during MPD in the later years. One of these methods is described in the paper Improved Kick Management During MPD by Real-Time Pore-Pressure Estimation by Gravdal et al. This paper describes a method for rapid estimation of porepressure after a gas kick. The method relies on detecting the turning point in a pressure-buildup curve. [8]

More data from additional equipment can be transferred faster than in the traditional way by mud-pulses, by use of new technology like wired-drillpipe telemetry.

MPD combined with new methods for detection of kick and loss and application of automatic tools can improve HSE and drilling efficiency. Some of the tools that MPD can benefit from have been used in other industries for a long time e.g. the PID-controller. [9, 10]

3.2.2. PID-controller

PID controller, short for Proportional-Integral-Derivative controller, is a generic control loop feedback mechanism widely used in industrial control systems. [10] The PID controller is used to minimize the difference between the desired setpoint (SP) and the measured process value (PV) by adjusting the process control inputs. In a PID controller there are 3 separate parameters: Proportional, Integration, and the Derivation term. [10]

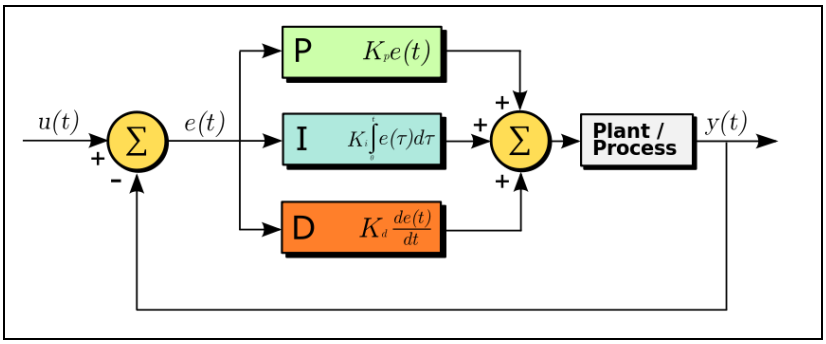

Figure 3.2.1: PID-controller block diagram. Taken from Wikipedia (PID controller) [10]

4. Experiments

All experiments are carried out on the experimental small scale test rig located at UiS. The rig is operated from the test laboratory using a computer with Matlab and Simulink. The rig was built by Magnus Tveit Torsvik and Alexander Wang who also wrote the control algorithms used to operate the rig. [1, 11]

Appendix A contains prints of the listed parameters for all experimental sets.

- Motor frequency
- Coriolis flowrate
- Standpipe pressure
- Downhole pressure
- MPD choke pressure
- Surface pressure

Operational controls in Simulink:

1) Pumprate: The pumprate is given as a fraction between 0 and 1 of the maximum motor speed at 50 Hz. 50 Hz corresponds to a maximum pumprate of 1400 litres pr. hour.
2) Influx time: The influx time is controlled automatically by setting the desired influx time interval in the Simulink model. The valve actuates from open to closed position and the other way around so quickly that it can be seen as instantaneous for our purposes.
3) Loss: The loss time is controlled automatically by setting the desired loss time interval in the Simulink model. Both loss valves require 10 seconds to change positions from open to closed and the other way around. The efflux cross sections are adjusted manually.
4) MPD choke opening: The MPD choke opening is given as a fraction between 0 and 1, where 0 is closed and 1 is fully open. This adjustment can be done manually or automatically using a PI-controller with a desired setpiont pressure, and using either downhole pressure or MPD choke pressure as reference pressure.

4.1. Conventional drilling

MPD open

In these experiments the MPD choke is fully open, which corresponds to a conventional drilling setup with annular flow return to open-to-atmospheric pressure.

4.1.1. No influx

1) MPD open, different pumprates.

Different pumprates give different flowrates, and the pressure responses to the different flowrates are shown in Figure 4.1 and Figure 4.2.

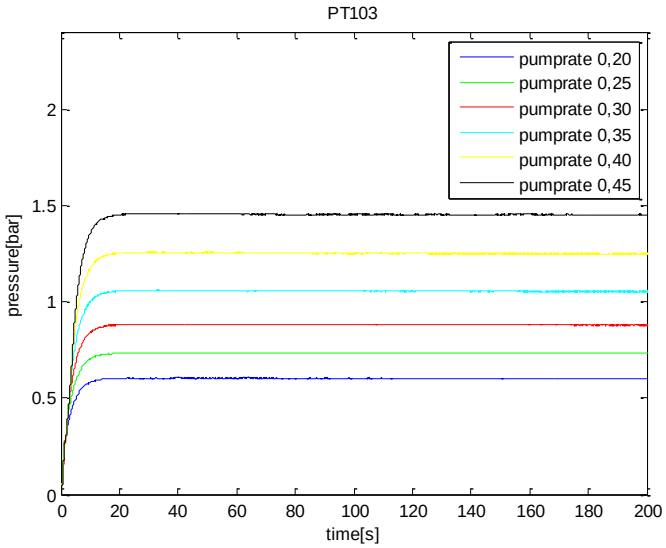

Figure 4.1: Downhole pressure as function of pumprate.

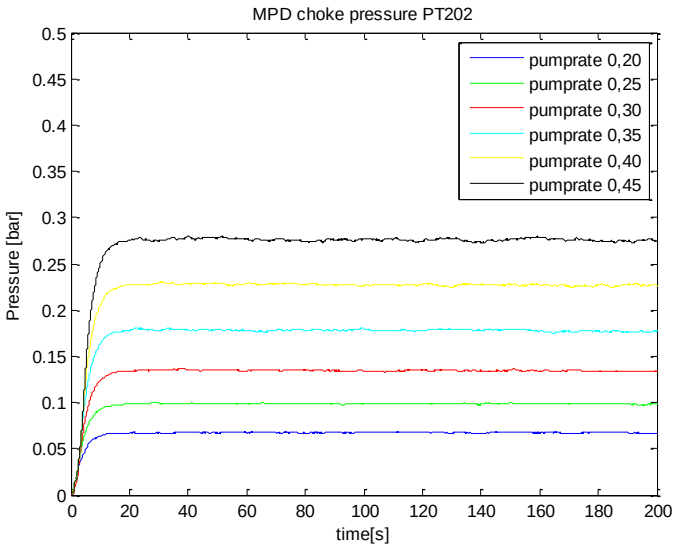

Figure 4.2: Topside pressure as function of pumprate.

Figure 4.1 and 4.2 show pressure responses to different flowrates. The pressure increases with higher flowrates due to the increased frictional forces. The pressure drop from downhole to the MPD choke can be found directly from the graphs by subtracting the readings in figure 4.2 from those in figure 4.1. The frictional pressure drop can be found by subtracting the hydrostatic pressure change from this result. The hydrostatic pressure change between downhole and topside is 0,4 bar.

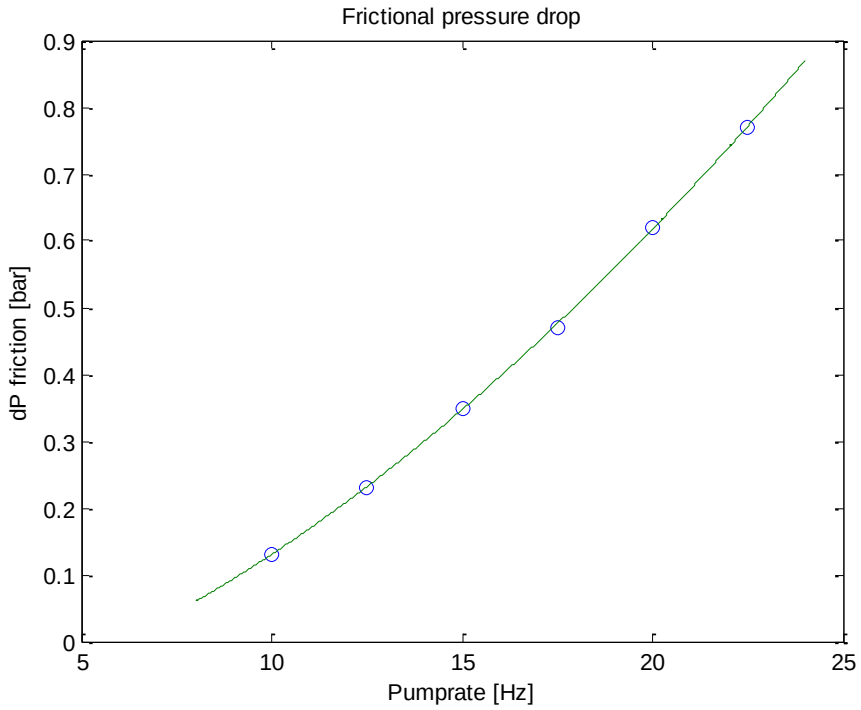

Figure 4.3: Frictional pressure drop as function of pumprate.

The plot in figure 4.3 is created in Matlab using polynomial regression analysis with the data obtained from the method described above. Only one datapoint from each of the six different pumprates are used in the analysis, and the plot is used for illustrative purposes only.

The pressure drop can also be calculated [12]

Single phase flow:

$$Re = \frac{\rho * u * D}{\mu}$$

$$f_t = 0,046 * Re^{-0,2} \qquad \text{(Dukler)} \qquad Re > 4000$$

$$f_l = \frac{16}{Re} \qquad \text{(Fanning)} \qquad Re < 2000$$

$$\frac{dP}{dx} = \frac{4}{D} * f * \frac{1}{2} * \rho * u^2 + \rho * g * h$$

Pipe length from the downhole pressure transmitter to the MPD choke pressure transmitter is approximately 57 meters.

$$\Delta P_{friction} = 57 * \left(\frac{4}{D} * f * \frac{1}{2} * \rho * u^2 \right)$$

The results are given in table 4.1. Appendix C includes Matlab calculations.

Pumprate	10	12,5	15	17,5	20	22,5
Calculated dP	0,1677	0,254	0,3515	0,4678	0,5968	0,7313
Measured dP	0,13	0,23	0,35	0,47	0,62	0,77
|dp1-dp2|	0,0377	0,024	0,0015	0,0022	0,0232	0,0387

Table 4.1: Frictional pressure loss, calculated and measured; as function of pumprate.

Measured and calculated values have been plotted together in figure 4.4 for comparison.

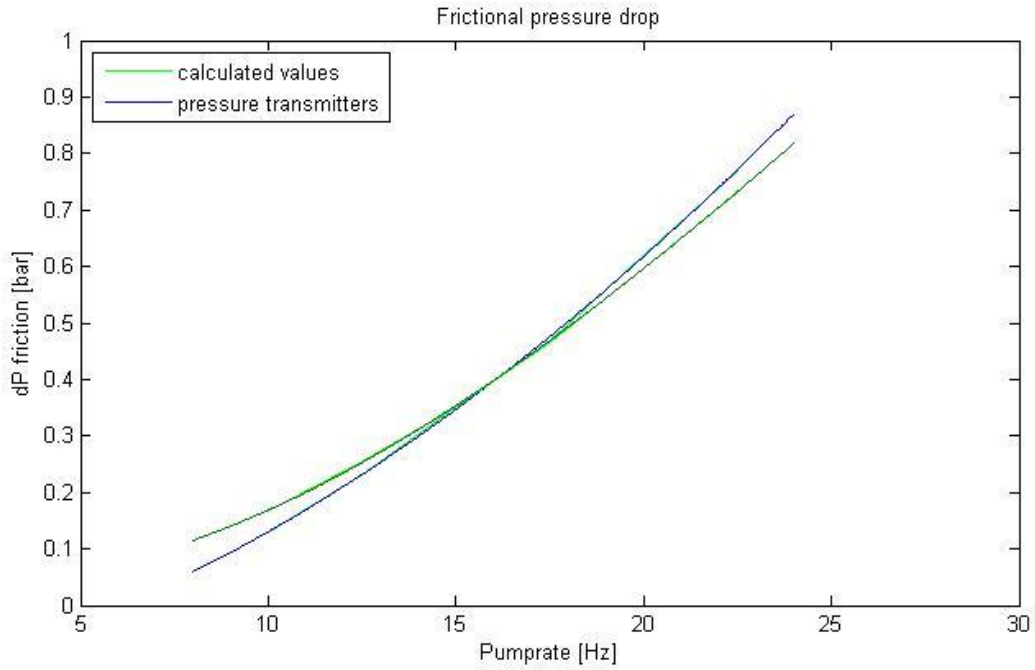

Figure 4.4: Measured- and calculated frictional pressure drop as function of pumprate.

The calculated friction model used here differs somewhat from the measured results obtained during tests. Possible improvements will be discussed in the next chapter.

4.1.2. Influx with large pressure margin

Kick size is determined by the pressure margin and the influx time. Adjusting a pressure reduction valve manually to a desired value to obtain a desired “pore” pressure, and adjusting the pumprate and MPD choke opening to obtain a desired “bottomhole” pressure, gives the pressure margin.

The listed experiments have been performed with 3,4 bar air pressure and MPD choke open:

2) Influx time 0,1 s, different pumprates
3) Influx time 0,2 s, different pumprates
4) Influx time 0,5 s, different pumprates
5) Influx time 1,0 s, different pumprates
6) Influx time 2,0 s, different pumprates
7) Influx time 3,0 s, different pumprates

Different influx times with air pressure 3,4 bar and constant pump pressure

In this section, we compare the plots for the different influx times for an arbitrarily chosen constant pumprate, here 12,5 Hz. The pumprate is kept constant at 25% of 50Hz which corresponds to approximately 3600 litres per hour. Six different influx times are plotted in the graphs Figure 4.5 and Figure 4.6. The air pressure is approximately 3,4 bar which is 2,7 bar higher than initial downhole pressure before kick initiation.

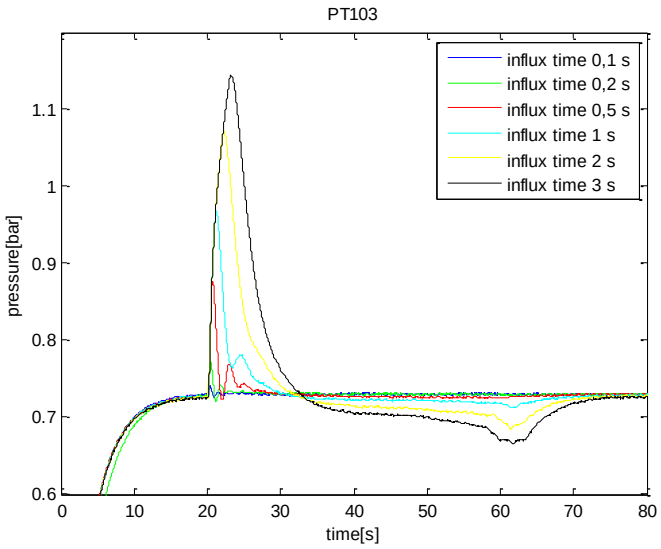

Figure 4.5: Downhole pressure response to different kick sizes with constant pumprate 0,25.

- t=0: the pump start and pressure build up in the system.
- t=15: pressure stabilizes
- t=20: gas kick is initiated

The pressure resonse is noticable for even the smallest influx time, and becomes significantly larger for each increment in influx time.

When the influx is stopped, the pressure decreases to a value that is lower than initial pressure before kick initiation. The pressure reduction is a combination of four different effects:

- Increased velocity (u) will result in a higher frictional pressure loss
- Lowering of the density (ρ) will reduce hydrostatic pressure
- Gasexpansion up the annulus
- Change in viscosity (μ)

The gas expansion effect is possible to detect for the larger influx times.

In this experiment the size of the kick is varied only by the influx time, and the reduction in pressure increases with larger kick sizes.

Figure 4.6 show topside flowrates. The Coriolis flowmeter measures mass flow [kg/hr], for fresh water this corresponds quite accurately to volume flow [l/hr], and since the Coriolis can only measure single phase flow, the measurements are only valid for the time before the gas enters the flowmeter.

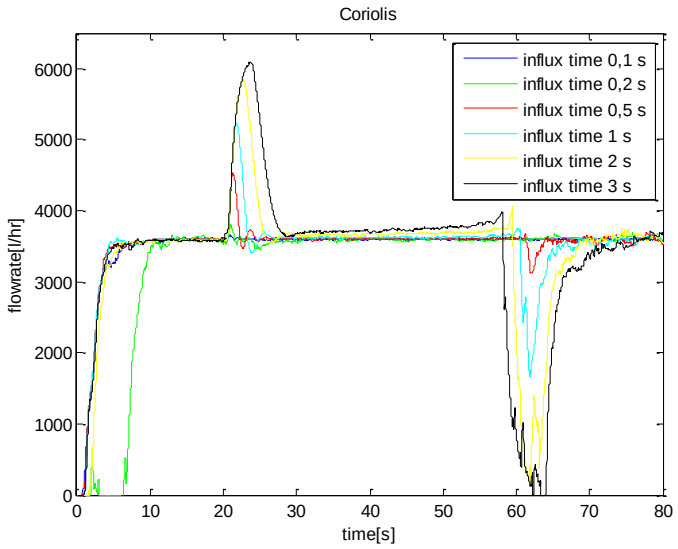

Figure 4.6: Topside flowrate through Coriolis with different kick sizes and constant pumprate 0,25.

Figure 4.6 shows that the flowrate is stabilizing around 3600 litres per hour before kick initiation at t=20s. As a result of the influx the flowrate will increase proportional to the amount of displaced water. After the influx has been stopped, the flowrate will start to decrease to a level where the flow rate corresponds to the initial flowrate in addition to the contribution from gas expansion. The contribution from gas expansion is seen most clearly for the larger kick sizes. When the gas enters the Coriolis flowmeter the measurements become distorted. This is clearly seen on the graph (from t=58s for influx time 3s.).

4.1.3. Influx with smaller pressure margin

The listed experiments have been performed with 2,0 bar air pressure and MPD choke open:

8) Influx time 0,2 s, different pumprates
9) Influx time 0,3 s, different pumprates
10) Influx time 0,4 s, different pumprates
11) Influx time 0,5 s, different pumprates
12) Influx time 0,6 s, different pumprates

Different influx times with air pressure 2 bar and constant pump pressure

The influx times from experiments 8-12 are plotted together for one pumprate. The pumprate is kept constant at 25%. Five different influx times are plotted in the graphs Figure 4.7 and Figure 4.8. The air pressure is approximately 2 bar which is 1,3 bar higher than initial downhole pressure before kick initiation.

Figure 4.7 show the pressure responses to different influx times, all with air pressure of 2 bar.

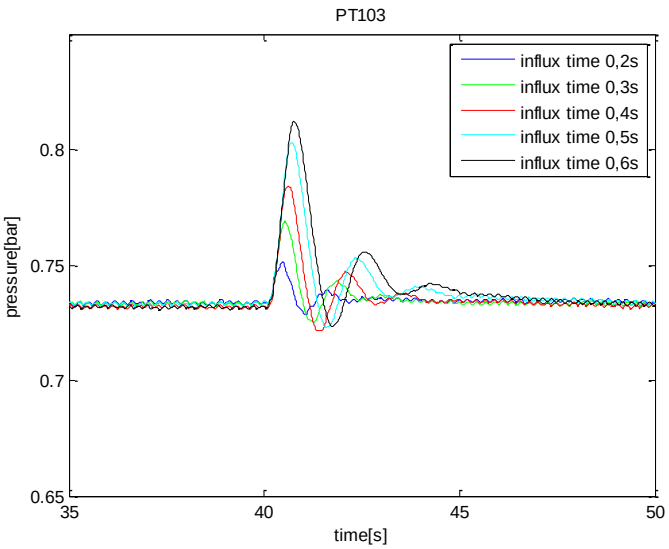

Figure 4.7: Downhole pressure response to different kick sizes with constant pumprate 0,25.

The influx start at t=40s, and as seen on the plot, the pressure response becomes more pronounced with increasing kick size. Influx times 0,2 and 0,5 in Figure 4.7 can be compared with the corresponding influx times from Figure 4.5. The pressure responses in Figure 4.5 are significantly larger than in Figure 4.7. The discrepancy is caused by the different air pressures.

Figure 4.8 show the flowmeter measurements for these experiments.

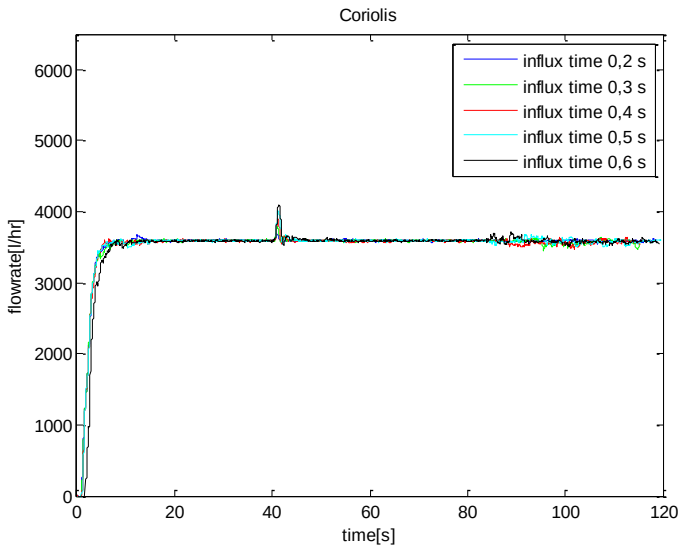

Figure 4.8: Flowrate through coriolis with different kick sizes and constant pumprate 0,25.

As for Figure 4.6, the flowrate increases proportional to the amount of displaced water during the influx. Here the influx is started at t=40s to ensure stabilized pressure in the system before kick initiation. The additional flowrates caused by the kicks are shown as flowrate spikes in the graph. The lowering of air pressure results in a lesser margin between PP and BHP, and hence reduction of the kick sizes. The gas enters the coriolis at approximately t=85-90s.

Figure 4.9&4.10 show the same influx times as Figure 4.7&4.8, plus one additional for influx time 1,2s. In Figure 4.9&4.10 the pumprate is 0,40.

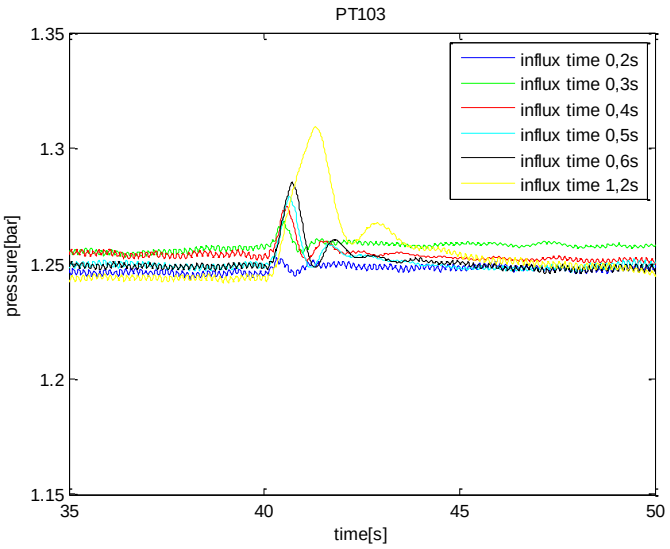

Figure 4.9: Downhole pressure response to different kick sizes with constant pumprate 0,40

The pressure response at PT103 for pumprate 0,40 is less than for a lower pumprate. This has two main reasons. Firstly, the flowrate is 60% higher here than in the last scenario and this gives a lower influx relative to the amount of total fluid flow. Secondly, the increased frictional forces results in a higher BHP while the PP remains the same which reduces the pressure margin and hence the size of the influx. The combined result of lesser kick sizes and increased BHP are a significant lowering of the relative pressure responses.

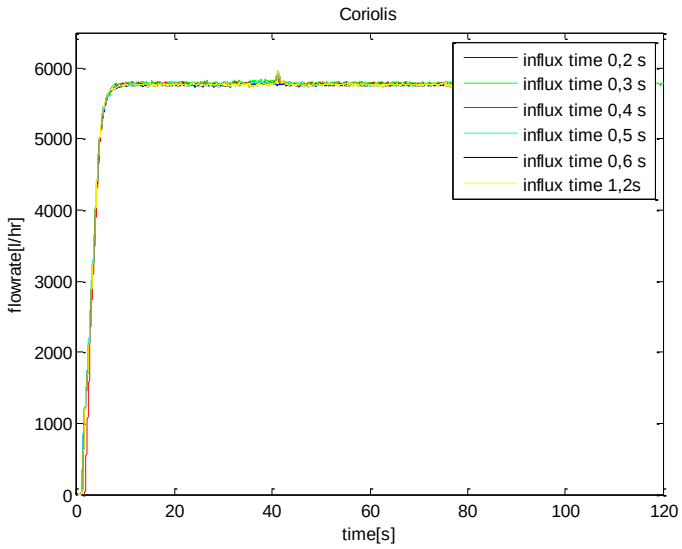

Figure 4.10: Flowrate through coriolis with different kick sizes and constant pumprate 0,40.

After influx initiation at t=40s, only minor spikes in total outflow are seen as in comparison with the graph shown in Figure 4.8.

4.2. Managed Pressure Drilling

MPD choke in use

In these experiments the MPD choke is in use. Firstly with a manually set choke to achieve an appropriate downhole pressure profile, later with an automated choke regulated by a PI-controller.

4.2.1. Manually set, constant choke

The listed experiments shows the effect of different influx times, and have been performed with the MPD choke in use to obtain a smaller pressure margin between PP and BHP, which allows longer influx time with smaller kick size:

13) MPD choke opening set to 0,507 to obtain a 0,3 bar pressure margin for pumprate 0,25
14) MPD choke opening set to 0,485 to obtain a 0,1 bar pressure margin for pumprate 0,25
15) MPD choke opening set to 0.730 to obtain a 0,1 bar pressure margin for pumprate 0,40

4.2.1.1. Different influx times with air pressure approximately 0,3 bar above bottomhole pressure and constant pumprate.

In these experiments the choke opening is kept constant at 50,7% with pumprate 0,25, to ensure a pressure margin of approximately 0,3 bar between BHP and PP.

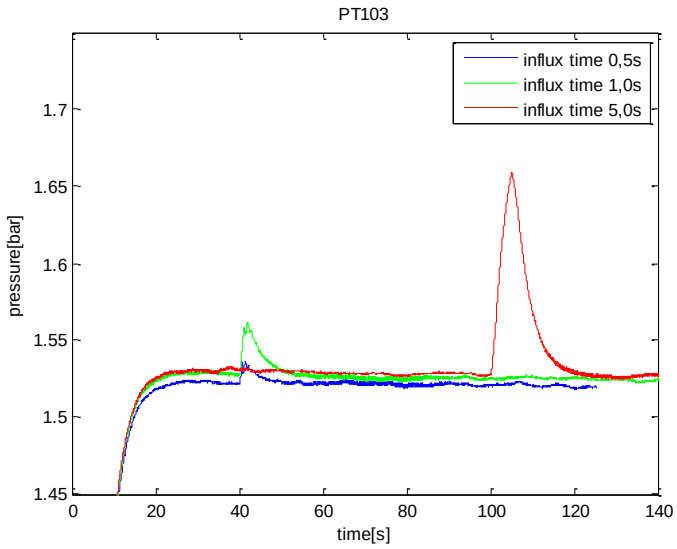

Figure 4.11: Downhole pressure response to different kick sizes with constant pumprate 0,25.

The two smaller kicks enter the well at t=40s, and the larger one enters the well at t=100s.

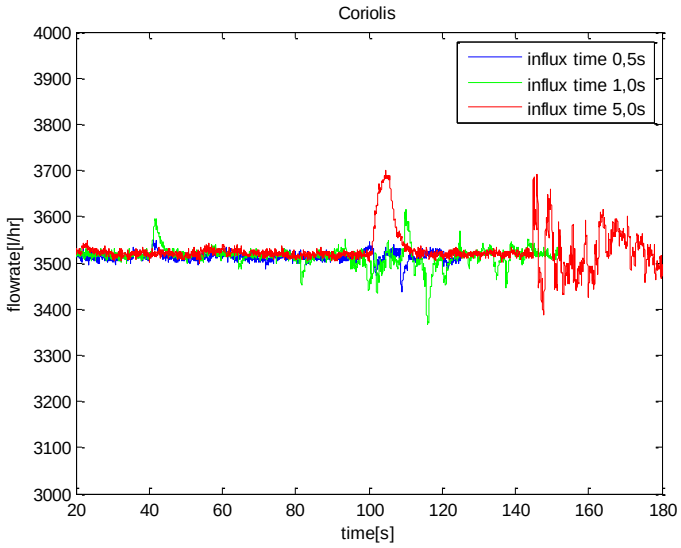

Figure 4.12: Flowrate through coriolis with different kick sizes and constant pumprate 0,25.

4.2.1.2. Different influx times with air pressure approximately 0,1 bar above bottomhole pressure and constant pump pressure.

In these experiments the choke opening is kept constant at 48,5% with pumprate 0,25, to ensure a pressure margin of approximately 0,1 bar between BHP and PP.

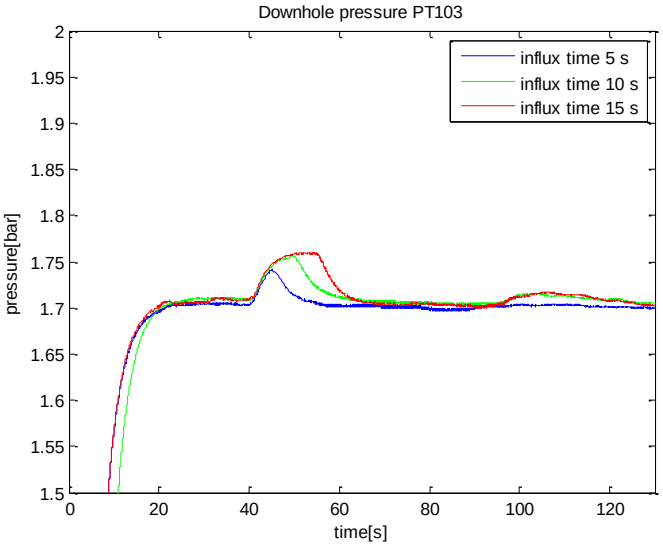

Figure 4.13: Downhole pressure response to different kick sizes with constant pumprate 0,25.

The pressure stabilizes around t=20, and influx is started at t=40.

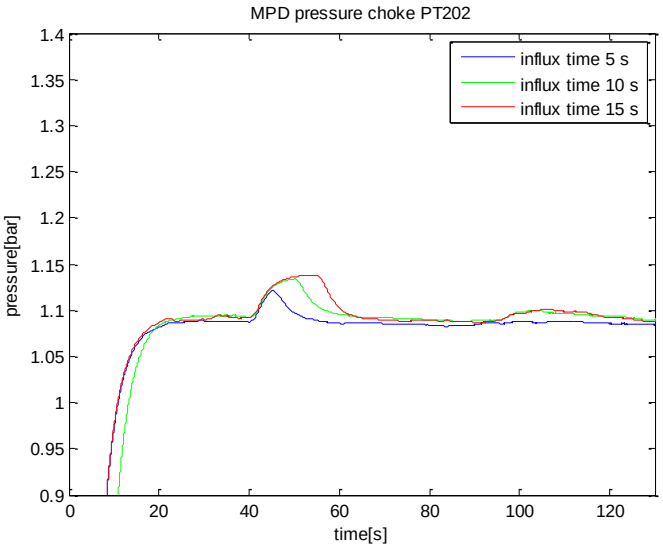

Figure 4.14: MPD pressure response to different kick sizes with constant pumprate 0,25.

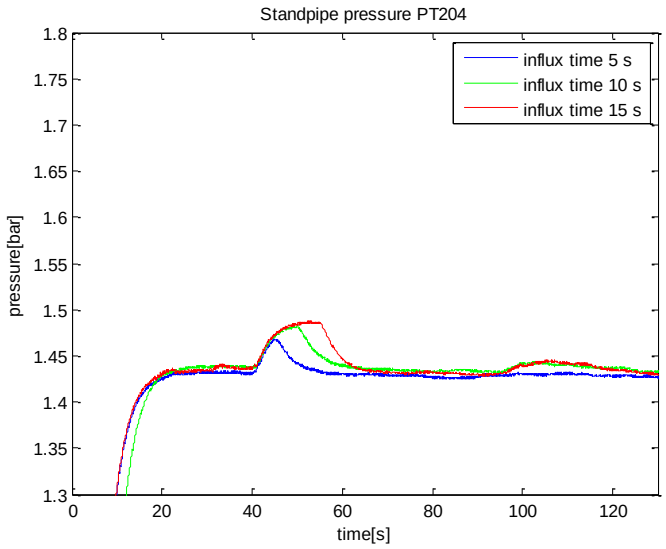

Figure 4.15: Standpipe pressure response to different kick sizes with constant pumprate 0,25.

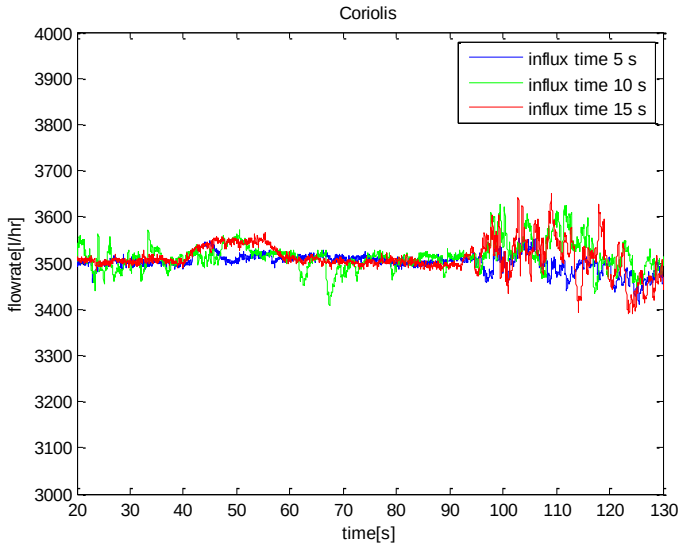

Figure 4.16: Flowrate through coriolis with different kick sizes and constant pumprate 0,25.

In Figure 4.16 the influx is hard to distinguish from the noise. The air pressure is barely above downhole pressure, and the influx enters the “well” as small intermittent waves of air bubbles. These small pulses of influx are enough to temporarily raise the bottomhole pressure to a level where the influx is stopped.

4.3. Loss

For all loss experiments, manual ball valves installed in front of the automatic "loss" valves have been used as provisional choke valves. The upper loss valve is denoted as A, while the lower is denoted B.

4.3.1. Loss without influx

The following loss without influx experiments has been performed:

16) Loss from A with different pumprates.
17) Loss from B with different pumprates.
18) Loss with pumprate 0,25 and MPD choke opening set to 0,485.
19) Loss with pumprate 0,25 and MPD choke opening set to 0,46.
20) Loss with pumprate 0,40 and MPD choke opening set to 0,73.
21) Loss with pumprate 0,40 and MPD choke opening set to 0,70.
22) Different loss sizes from A with pumprate 0,30.
23) Different loss sizes from B with pumprate 0,30.

For experiment 16-21 the "loss valve" opening was kept constant.

For the two first experiments the MPD choke was set to 0,73. See appendix A (16 & 17).

Figure 4.17 and 4.18 show coriolis flowrate and downhole pressure response respectively, for the "loss with pumprate 0,25 and MPD choke opening set to 0,46" experimental set (19). The pressure response is proportional to the loss. From the coriolis readings we can determine the loss to be approximately 1,7% for valve A, 1,4% for valve B, and 3,1% combined. The corresponding reduction in pressure is 4,3% for A, 3,4% for B, and 7,7% for the case where both valves are open at the same time. The experimental set (18) yields similar results. As seen from data collected from experimental set 20 & 21, higher pumprates than 0,25 will not lead to additional loss. Consequently, the relative loss becomes smaller with increasing pumprate.

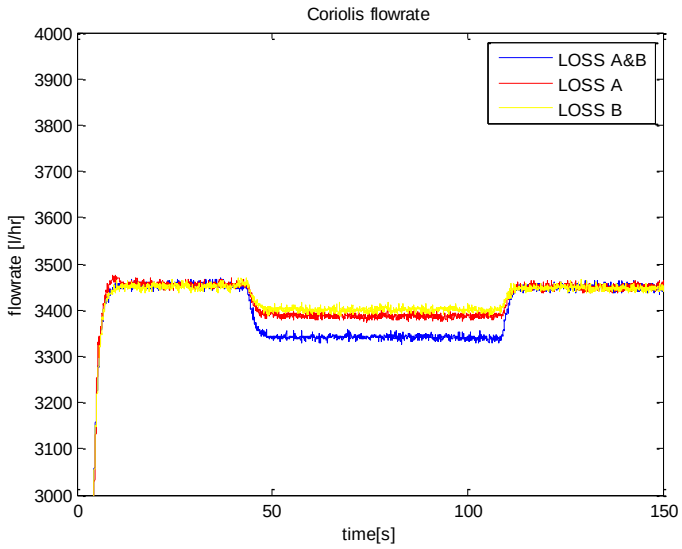

Figure 4.17: Lost circulation. Loss valves open in the interval t ϵ [40,100]

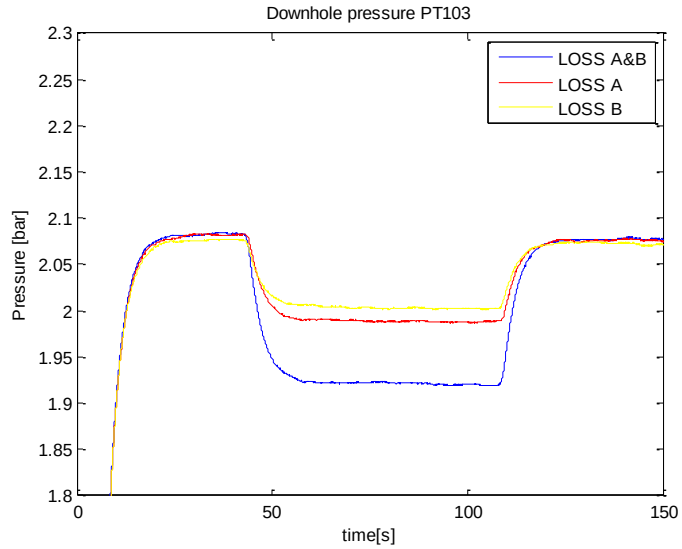

Figure 4.18: Downhole pressure response to lost circulation in the interval t ϵ [40,100]

Figure 4.19 and 4.20 show coriolis flowrate and downhole pressure respectively, for experimental set 23: Different loss sizes from lower loss valve with pumprate 0,30.

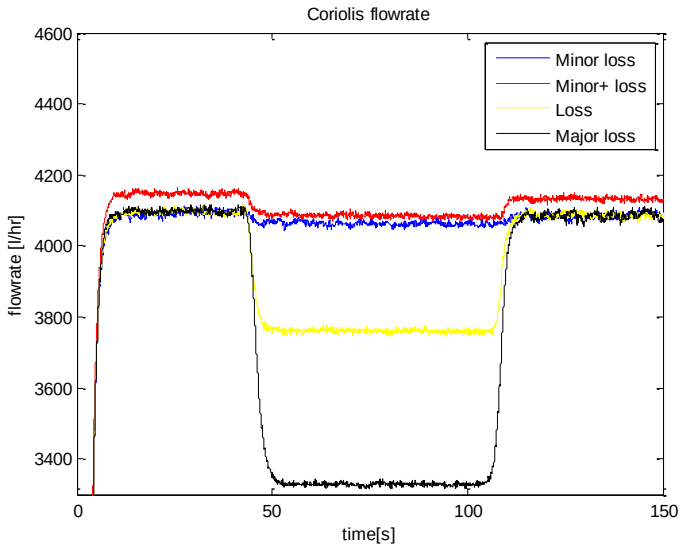

Figure 4.19: Lost circulation size for different loss valve openings.

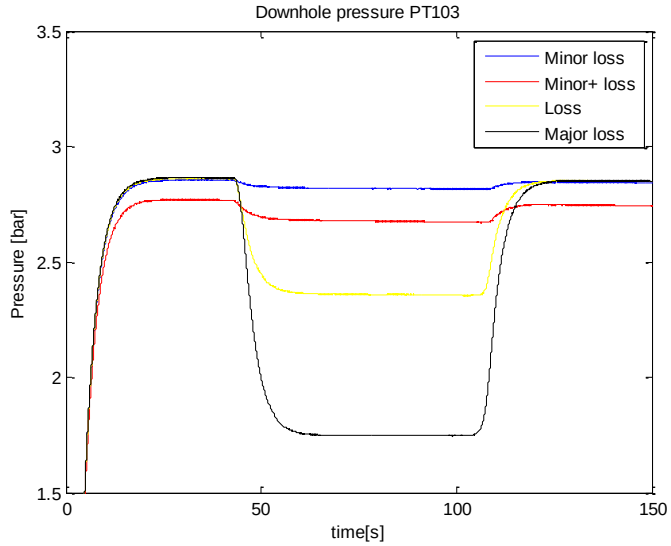

Figure 4.20: Downhole pressure response to different loss valve openings.

The results from these experiments give the following relative lost circulation data:

	Relative changes in:	
	Coriolis flowrate	Downhole pressure
Minor loss	< 1%	≈ 1%
Minor+ loss	≈ 1%	≈ 3%
Loss	≈ 8%	≈ 17%
Major loss	≈ 19%	≈ 35%

Table 4.2: Downhole pressure response to different lost circulation scenarios.

The downhole pressure response is not unique; all the other pressure transmitters from the pump to the MPD choke have similar characteristics.

There is an unanticipated difference between the minor+ loss experiment and the three others. A possible reason for this discrepancy will be treated in the discussion chapter.

4.3.2. Loss-induced kick

Two experiments were performed with loss-induced kick:

24) Loss from B inducing kick.
25) Loss from A&B inducing kick.

A constant pumprate and MPD choke opening will provide a stable pressure in the system. As seen from the previous experiments, efflux through loss valves will lead to a pressure drop that is proportional to the lost circulation. In the experiments in this subchapter, the downhole pressure transmitter (PT103) is used as reference in the Simulink model. When the downhole pressure gets below 2 bar, air influx is initiated.

The loss valves opens at t=40s and closes at t=100s. Figure 4.21 show the downhole pressure during experiment 25: Loss from upper and lower loss valve inducing kick.

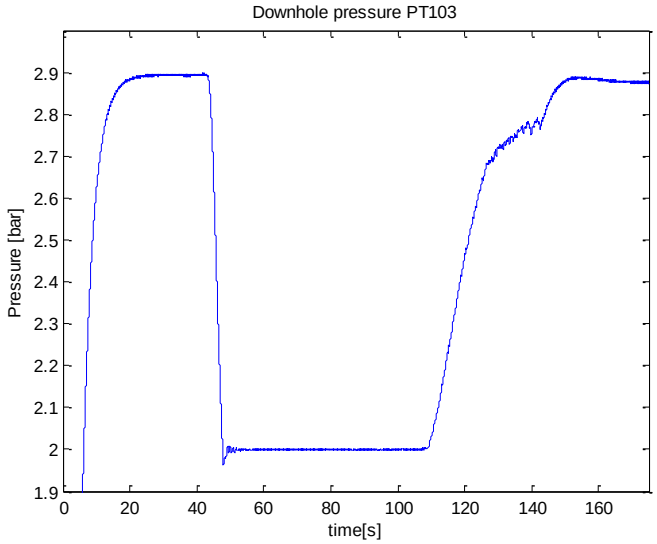

Figure 4.21: Downhole pressure during loss-induced kick experiment.

After valves A&B open, the pressure plunges below 2 bar, and the influx starts. The pressure oscillates around 2 bar due to the commands:

- Downhole pressure < 2 bar: Influx
- Downhole pressure > 2 bar: No influx

4.4. MPD automatic choke

During these experiments a PI-controller was used to regulate the MPD choke automatically. PT 202 were used as reference pressure with setpoint 1,0 bar. Influx starts at t=100s and ends at t=105s. Air pressure is approximately 0,3 bar higher than downhole pressure.

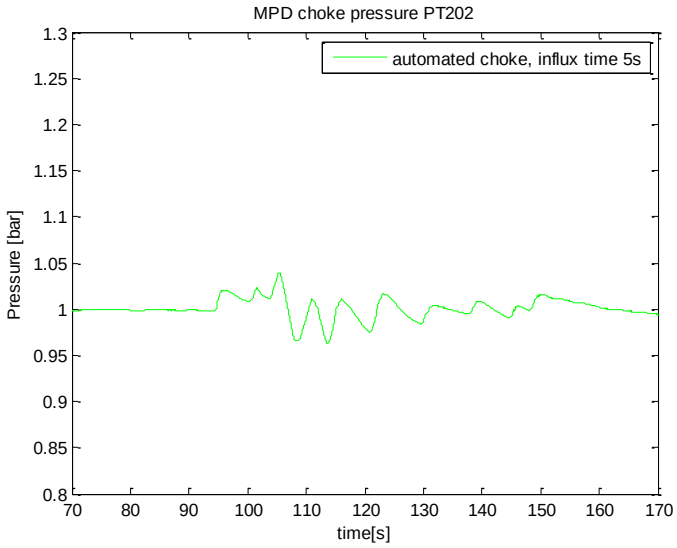

Figure 4.22: Pressure response to kick with automated MPD choke.

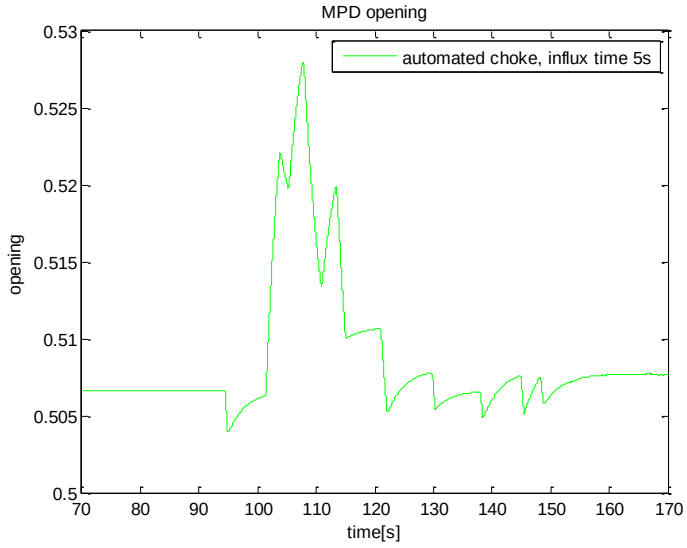

Figure 4.23: MPD choke opening response using PT202 as reference.

MPD choke opening is automatically adjusted to keep the topside pressure at 1 bar. The deviation from setpoint is less than 0,05 bar.

5. Discussion

The small scale test rig cannot realistically give an account of all aspects of a drilling operation. It operates at low pressures, the difference in height from the pump to MPD choke and Coriolis flowmeter is 4,5 meters, and the total length from the pump to the Coriolis is 72 meters. The pressure response will be very fast in a small scale test compared with in a real well. Also, since the gas is injected only four meters below "top side", the hydrostatic pressure difference is only 0,4 bar, and the influx experiments pressure responses will represent only what happens in the uppermost part of the well where most of the gas expansion has already taken place in a real case scenario.

The pump that is used with the test-rig will provide a predetermined flowrate, and will not be affected by changes in pressure caused by gain or loss.

When the MPD choke is open we can clearly see that the flowrate measured in the Coriolis will respond immediately to a kick. The increase in outflow will correspond to the displacement of water by air influx. The pressure response in the well will increase in accordance with the gain.

When the MPD choke is used to obtain a BHP closer to the PP, we can see that the pressure responses in the well will give a clearer indication of kick than the gain measured by the Coriolis. An example of this is the plots in figures 4.13-16.

In order to simulate scenarios with Matlab and then testing them in the rig, a model for the fluid dynamics in the rig needs to be developed. In chapter 4.1.1 an attempt was made to calculate frictional pressure drop and comparing it with experimental data. The calculation model overestimates frictional pressure drop for low pumprates and underestimates it for high pumprates, compared to the measured values. The constructional form of the small scale rig is of importance here. The pipeline has dozens of ninety degree bends over a relatively short distance, and this will affect the dynamics of the flow. Modifications in the calculation model can be made to better fit experimental data.

A gas meter can be installed on the air side for measurement of influx in order to accurately determine kick size.

Some of the experiments provide data with a higher degree of "noise" than others. As a general rule, less "noise" was experienced during evenings and in weekends. This gives reason to believe the rig is picking up interference from other activity in the building. Another, and more severe form of "noise", is that of trapped air in pipe bends, which is then released at any random time. It is difficult to say when or how much air from influx trapped in pipe bends will be released, but when some bubbles are released, the bubbles often drives out additional air from each passing bend.

The ball valves installed in front of the loss valves are not well suited to function as choke valves. The choke openings are set manually to allow flow passage by partial opening of the ball valves. These experiments will therefore have reduced reproducibility. However, the test rig operates on relatively low pressures and flowrates, and the ball valve positions were apparently not changed considerably while the experiments were conducted.

With increasing pumprate the relative loss becomes smaller. The loss outlets are smaller diameter pipes located at the underside of the main pipe. Increased velocity in the main pipe will lead to a much higher increase in velocity through the small cross-section area of the partially open loss valves. Increase in velocity leads to higher pressure drop over the valve. The pressure build-up in front of the valve balances that of extra friction in the main pipe plus the pressure build-up in front of the MPD choke valve.

There is an unanticipated difference between the minor+ loss experiment and the three others, as mentioned in chapter 4.3.1. No leaks from the system were detected. One likely explanation for the discrepancy is that the pressure relief valve activated and bled of the amount of water that make up the difference between the measured coriolis flowrate for the minor+ loss case and the three others. This statement is supported by the printout of the motor frequency for this experimental set, figure 5.1, where pumprate for the minor+ case is impossible to distinguish from the others, and also from the MPD choke opening printouts, figure 5.2&5.3. The MPD choke, even when it is manually set to one specific value, sometimes adjust the choke opening a little "by itself". As seen on figure 5.2, it is difficult to distinguish the four graphs from each other, but if we zoom in on the vertical axis, as seen in

figure 5.3, the difference become apparent. We can read from figure 5.3 that the minor+ loss experiment were performed with MPD choke 0,2% more open than the other three.

The pressure relief valve is placed right after the pump since the highest pressure in the system is experienced here due to the frictional forces. Pressure transmitter PT101 is also placed here. If we now look at the printout of the pump pressure, figure 5.4, we can see that the 0,2% choke opening increase results in a 0,1 bar lower pump pressure. It is reasonable to believe that the pressure safety valve starts to bleed of when the pressure reaches approximately 3.15 bar, as figure 5.4 suggest.

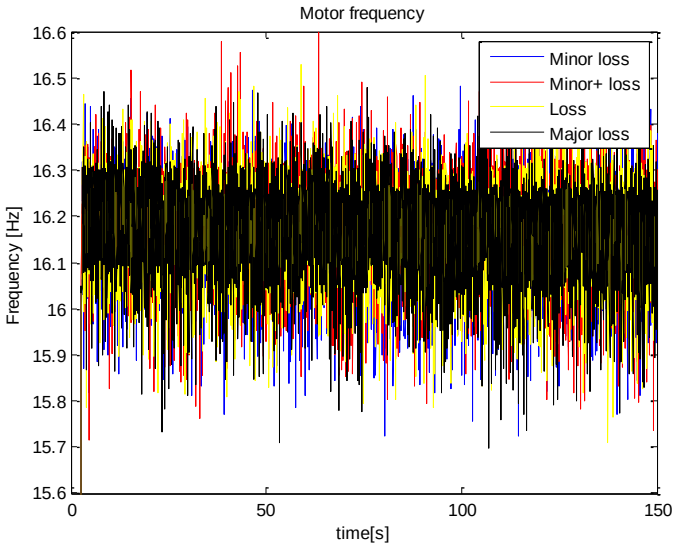

Figure 5.1: Motor frequency.

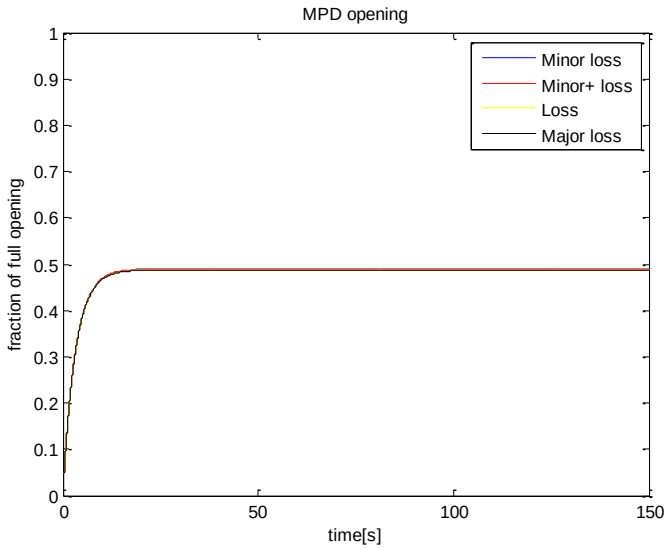

Figure 5.2: MPD choke opening.

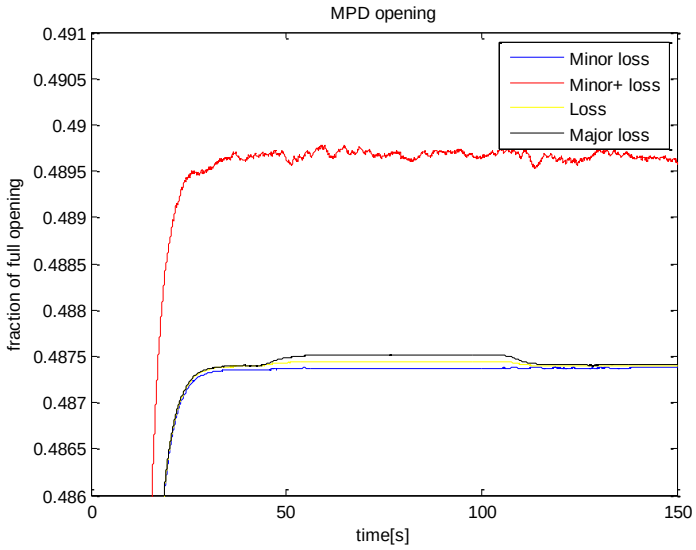

Figure 5.3: MPD choke opening, zoom-in on vertical axis.

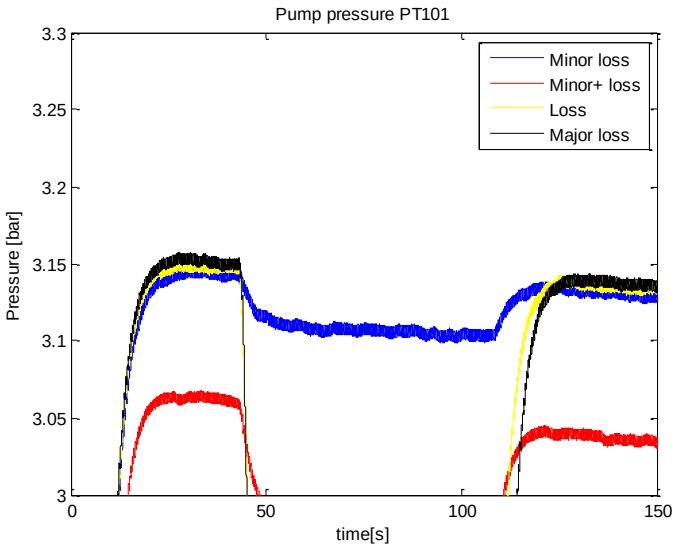

Figure 5.4: Measured pressure close to the safety valve.

6. Conclusion and further work

For every experiment, pressure responses in the system are closely related to changes in flowrate measured by the Coriolis. In most cases the pressure transmitters measure a larger relative change in pressure compared to the relative change in flowrate. This indicates that monitoring pressure changes in the system, be it standpipe, downhole, or MPD choke pressure, can be an effective way to detect gain- or loss situations. Furthermore, pressure readings will continue to be valid even when the Coriolis is disabled during two-phase flow. This is of importance in possible future experiments performed on the rig, as longer influx times with a small pressure margin are more in harmony with a real well.

More work should be done with respect to obtaining a hydraulic model that fits better with the data collected from experiments, in order to simulate different scenarios and then test them at the rig. Differential pressure cells have now been installed on the rig. Experiments without gain or loss can be reproduced easily - several directly comparable datasets should be collected in order to build a friction model that more accurately represents the small scale rig.

Kick size estimation is of importance when evaluating an influx situation. The kick size is determined by pressure margin and influx time. A gas flowmeter can be installed on the air side for measurement of influx in order to accurately determine kick size.

The ball valves used as loss flow choke valves can advantageously be replaced with automatically controlled flow control valves.

7. References

1. Wang, A., *MPD og automatisk brønnsparkhåndtering anvendt på boreriggmodell*. 2012, A. Wang: Stavanger.
2. Aadnøy, B.S., *Advanced drilling and well technology*. 2009, Society of Petroleum Engineers: Richardson, Tex. p. 750-763.
3. Nauduri, S., G.H. Medley, and J. Schubert, *MPD Candidate Identification: To MPD or Not To MPD*, in *SPE/IADC Managed Pressure Drilling and Underbalanced Operations Conference and Exhibition*. 2010, SPE/IADC Managed Pressure Drilling and Underbalanced Operations Conference and Exhibition: Kuala Lumpur, Malaysia.
4. Bourgoyne, A.T., *Applied drilling engineering*. SPE textbook series. Vol. Vol. 2. 1986, Richardson, TX: Society of Petroleum Engineers. VI, 502 s.
5. Aadnøy, B.S., *Mechanics of Drilling*. 2006: Shaker Verlag.
6. Al-hamhami, S.S., et al., *First Successful Implementation of MPD Technology in PDO (Sultanate of Oman) to Mitigate Drilling Hazards*, in *SPE/IADC Middle East Drilling Technology Conference and Exhibition*. 2011, SPE/IADC Middle East Drilling Technology Conference and Exhibition: Muscat, Oman.
7. Santos, H.M., et al., *First Field Applications of Microflux Control Show Very Positive Surprises*, in *IADC/SPE Managed Pressure Drilling & Underbalanced Operations*. 2007, 2007 IADC/SPE Managed Pressure Drilling and Underbalanced Operations Conference and Exhibition: Galveston, Texas, U.S.A.
8. Gravdal, J.E., et al., *Improved Kick Management During MPD by Real-Time Pore-Pressure Estimation*, in *SPE Annual Technical Conference and Exhibition*. 2009, Society of Petroleum Engineers: New Orleans, Louisiana.
9. Godhavn, J.-m. and K.A. Knudsen, *High Performance and Reliability for MPD Control System Ensured by Extensive Testing*, in *IADC/SPE Drilling Conference and Exhibition*. 2010, 2010, IADC/SPE Drilling Conference and Exhibition: New Orleans, Louisiana, USA.
10. *PID controller*. 2012 06.03.2012 [cited 2012 19.03.2012]; Available from: http://en.wikipedia.org/wiki/PID_controller.
11. Torsvik, M.T., *Laboratoriemodell av boreprosess. Bygging: instrumentering, igangkjøring og regulering*. 2011, M. T. Torsvik: Stavanger.
12. Time, R.W., *Multiphase flow in pipes, compendium MPE 700, chapter 2.* 2009.

Appendix A

Experimental plots

1) Experimental data for different pumprates with MPD open without influx

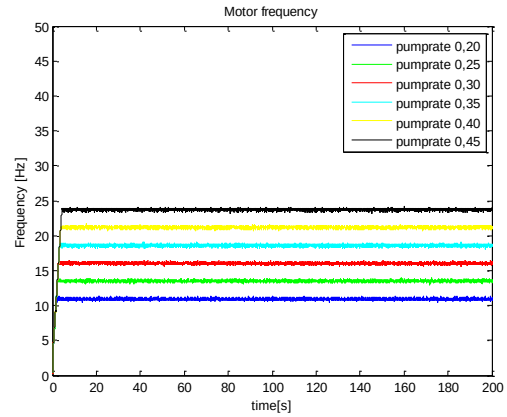

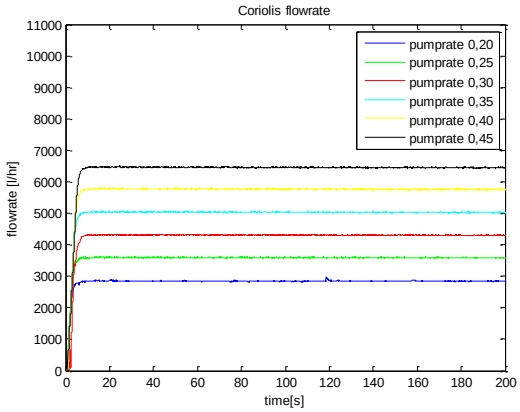

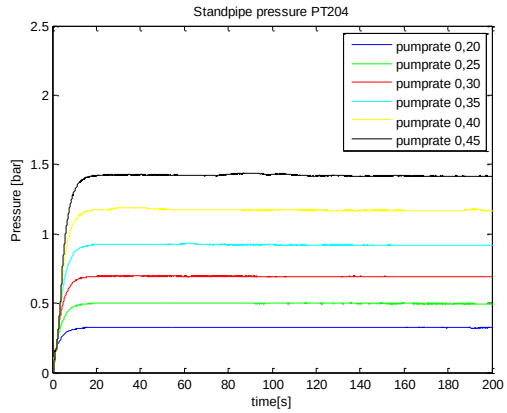

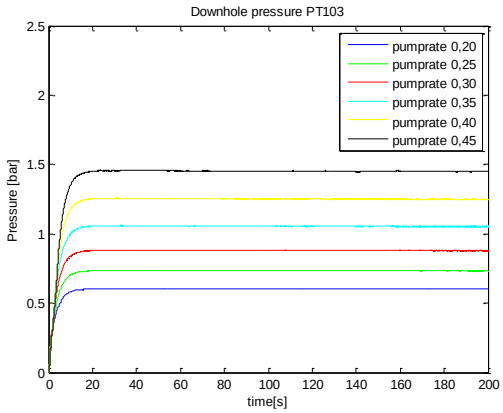

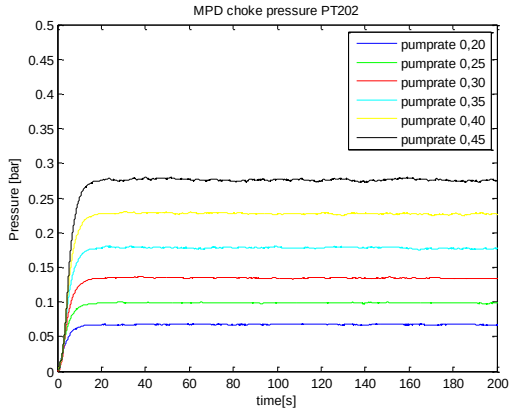

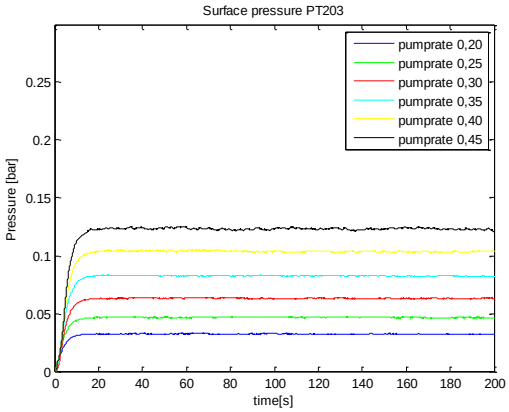

For 2-7: Air pressure 3,4 bar. Influx at t=20s.

2) Experimental data for different pumprates with MPD choke open and influx 0,1 seconds with air pressure 3,4 bar.

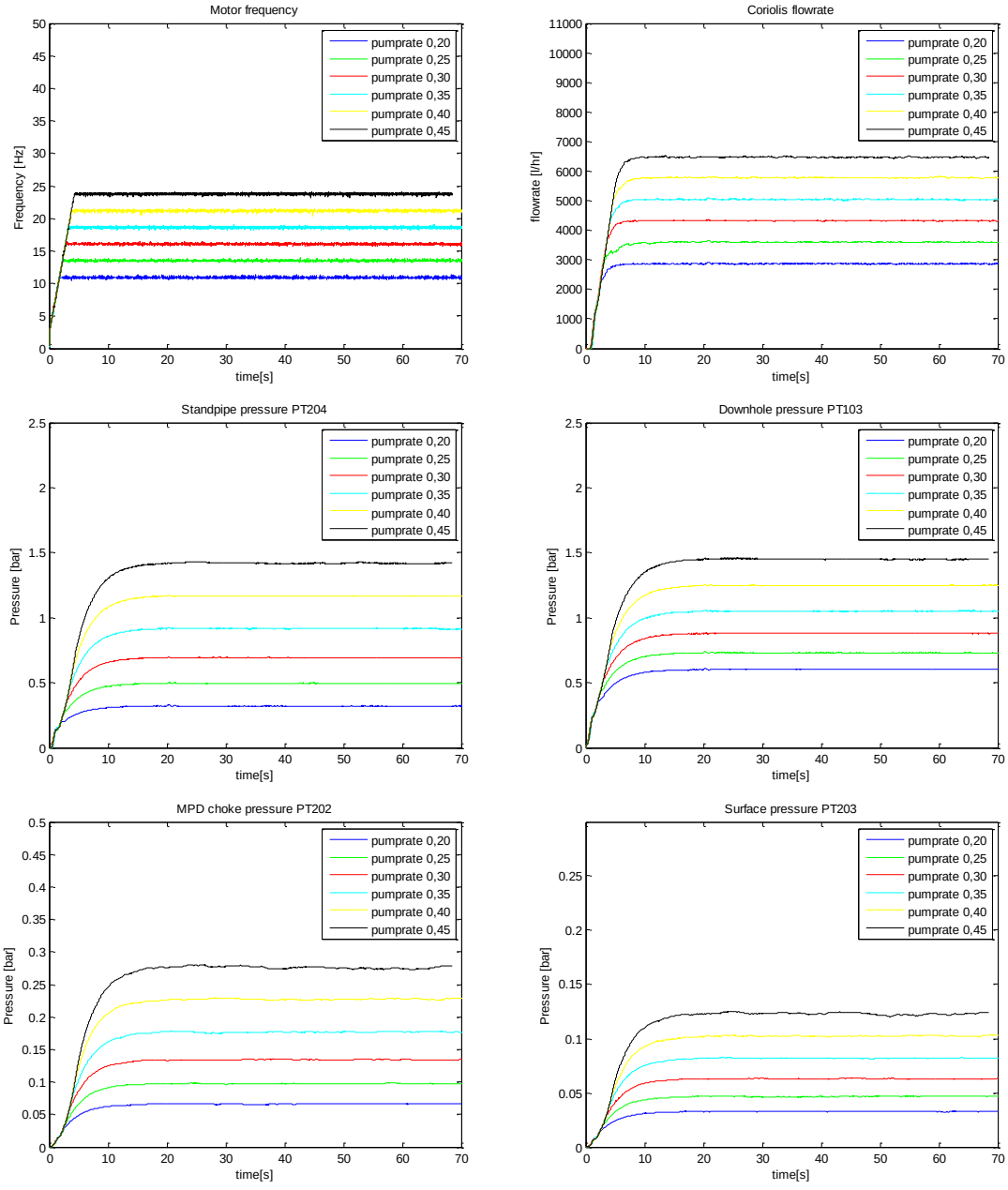

3) Experimental data for different pumprates with MPD choke open and influx 0,2 seconds with air pressure 3,4 bar.

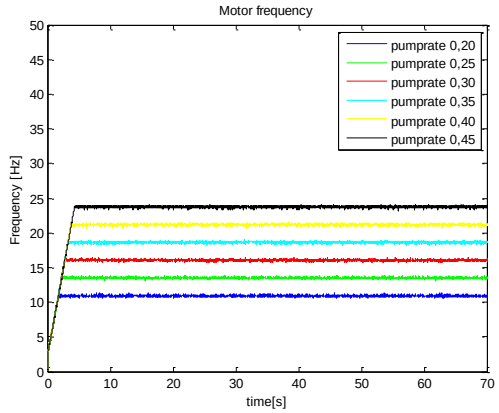

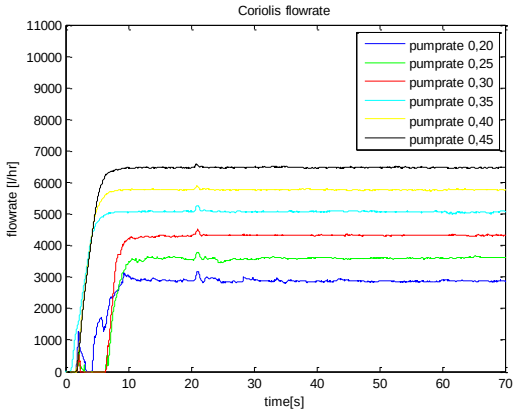

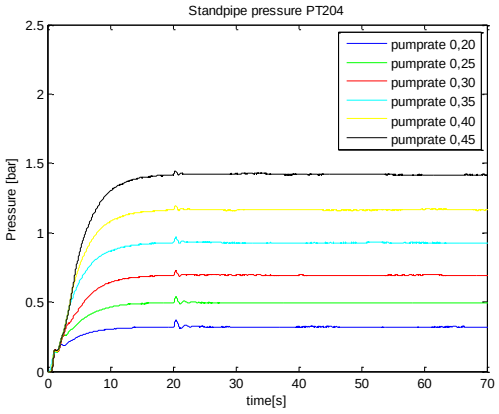

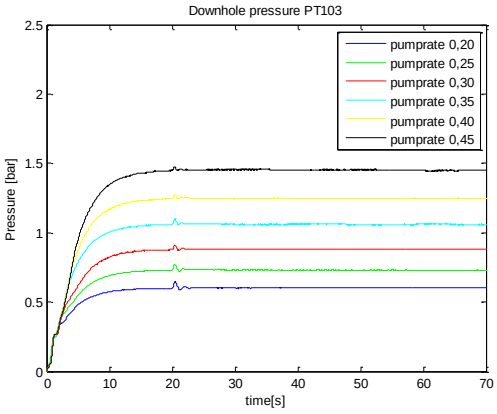

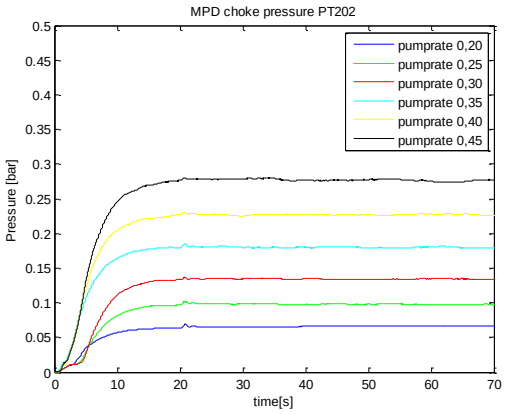

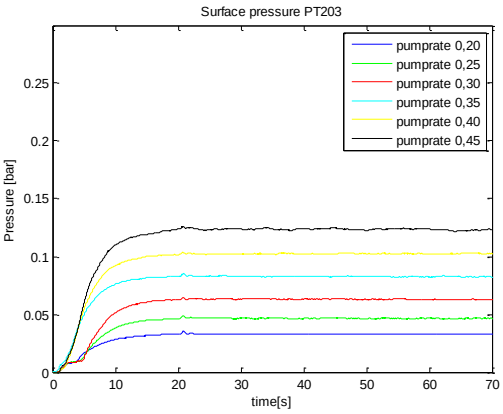

4) Experimental data for different pumprates with MPD choke open and influx 0,5 seconds with air pressure 3,4 bar.

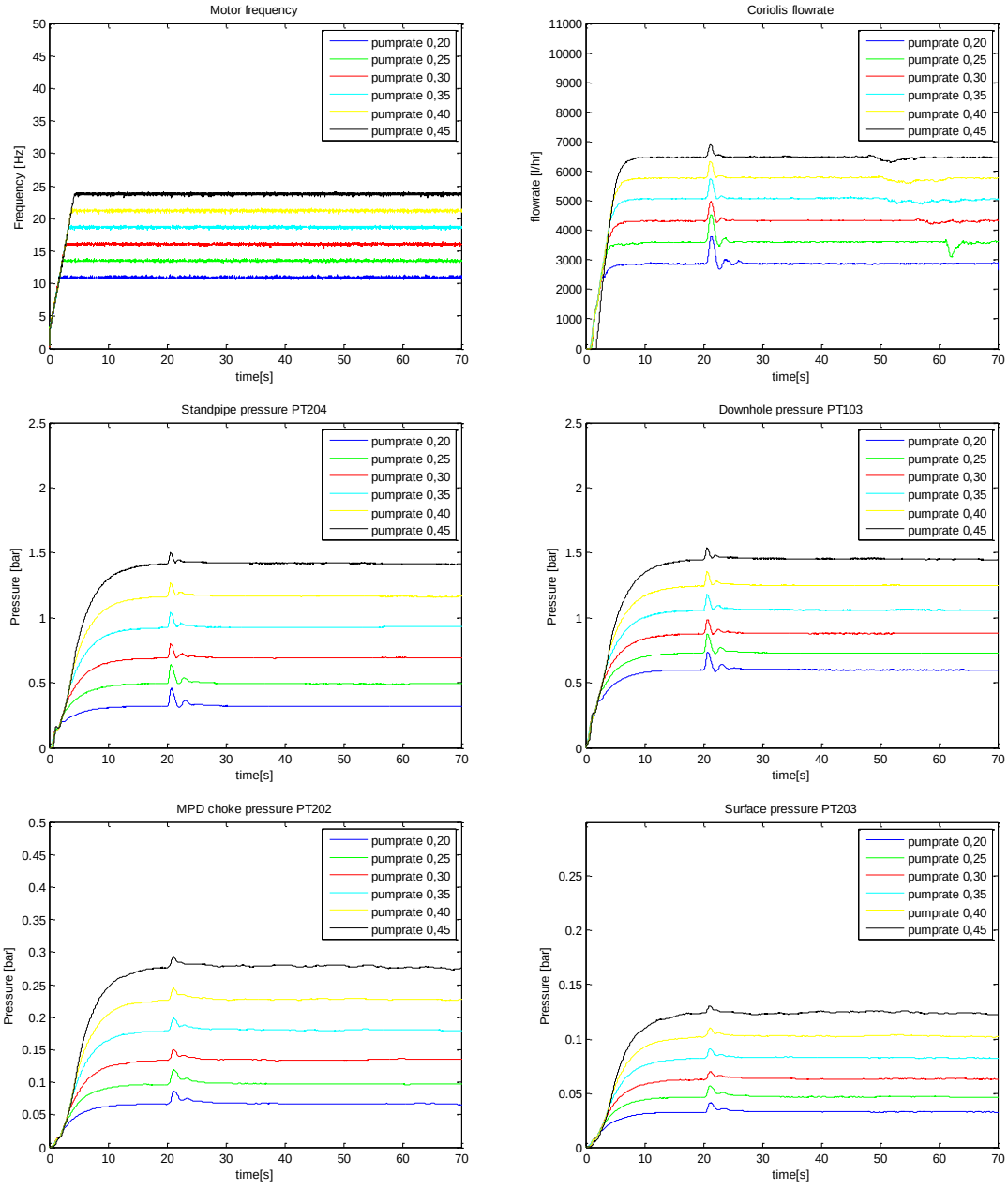

5) Experimental data for different pumprates with MPD choke open and influx 1 second with air pressure 3,4 bar.

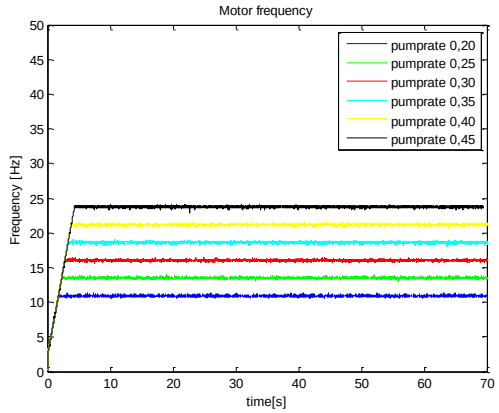

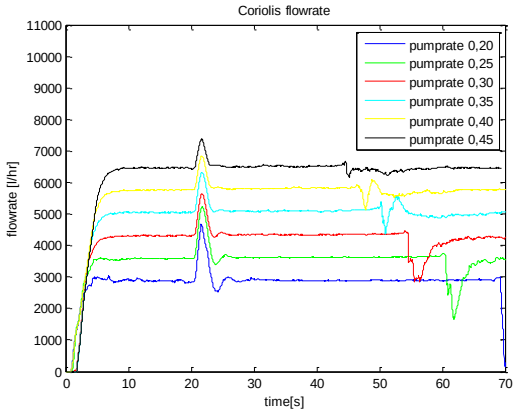

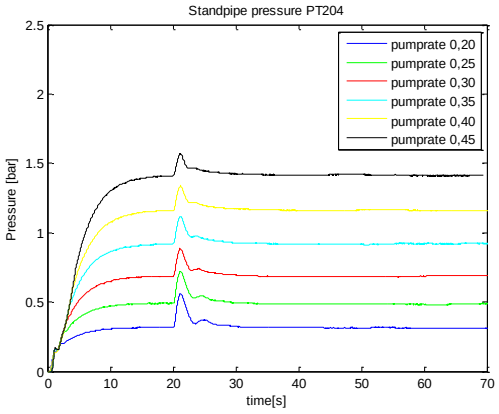

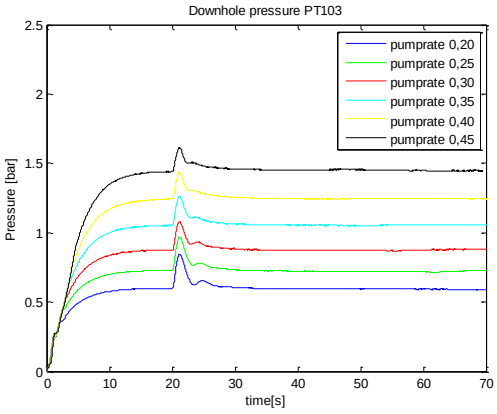

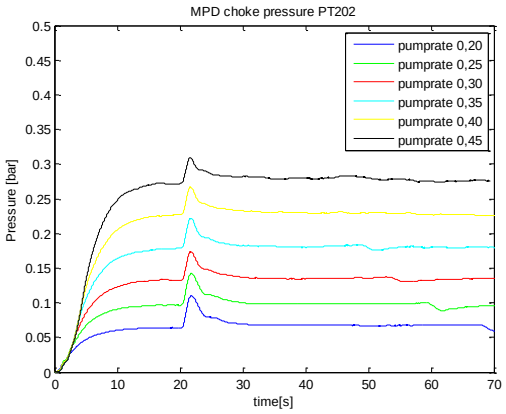

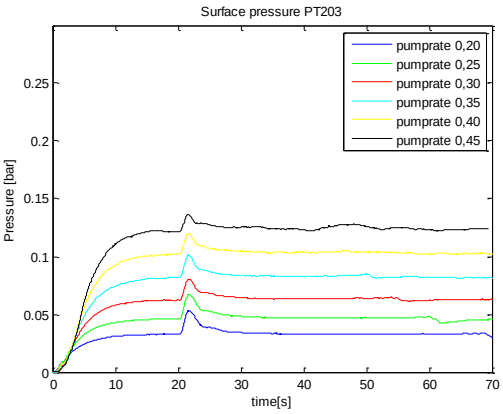

6) Experimental data for different pumprates with MPD choke open and influx 2 seconds with air pressure 3,4 bar.

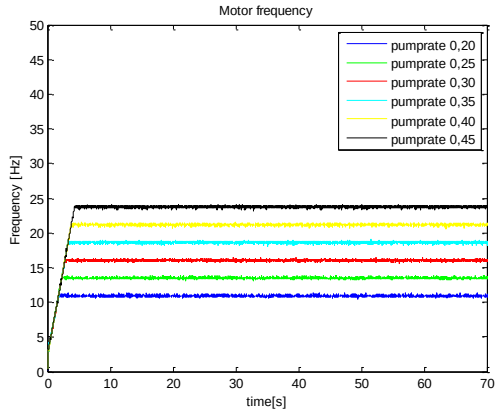

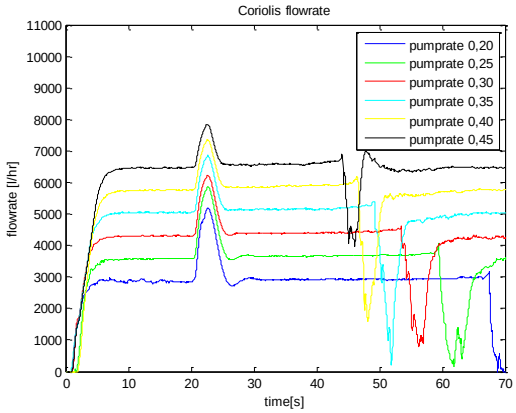

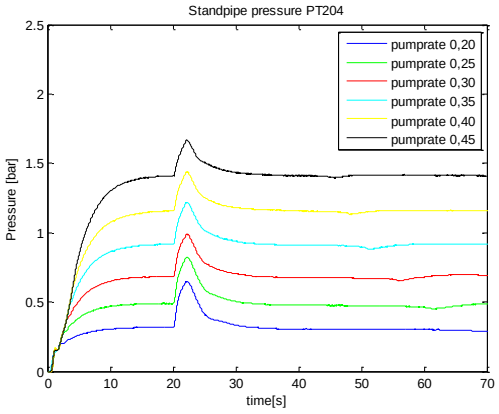

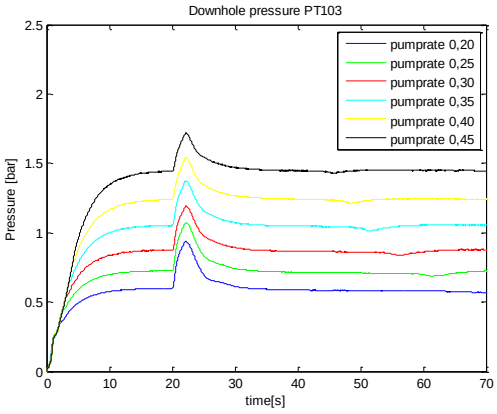

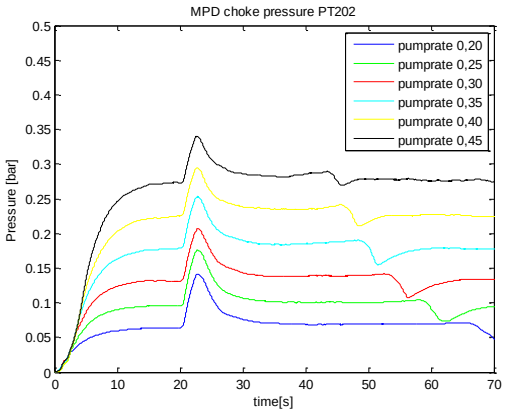

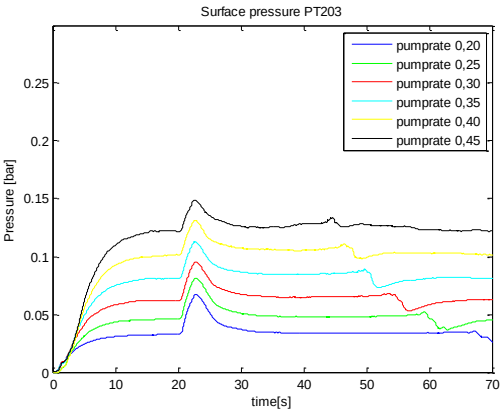

7) Experimental data for different pumprates with MPD choke open and influx 3 seconds with air pressure 3,4 bar.

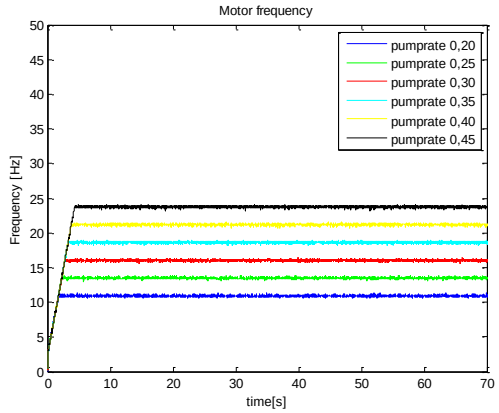

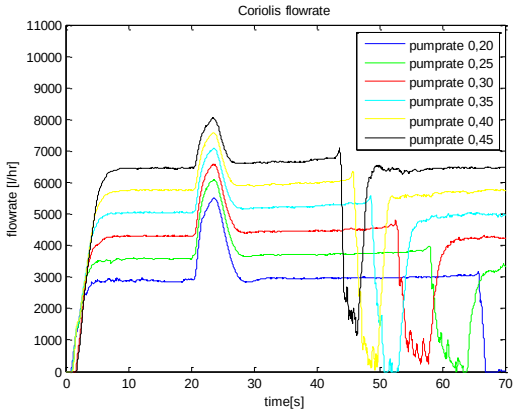

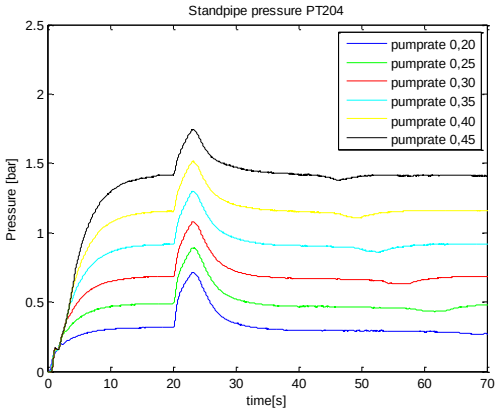

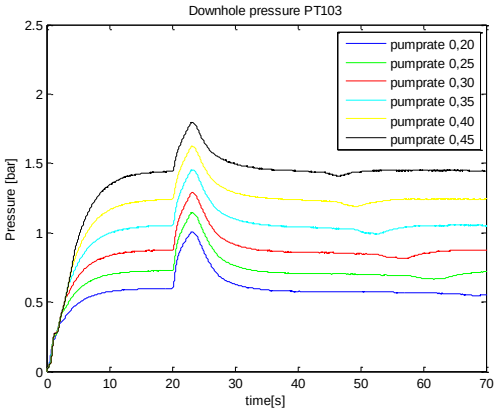

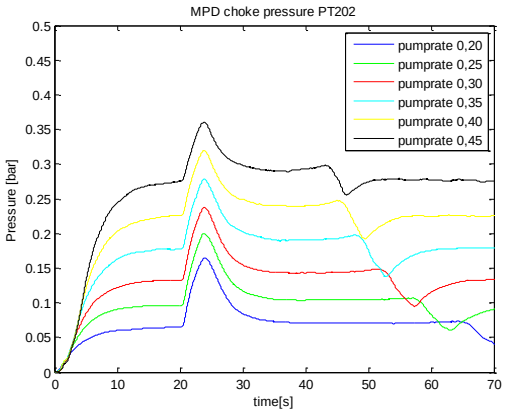

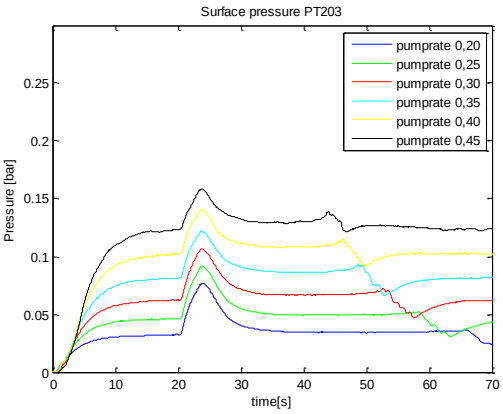

For 8-12: Air pressure 2 bar. Influx after 40s.

8) Experimental data for different pumprates with MPD choke open and influx 0,2 seconds with air pressure 2 bar.

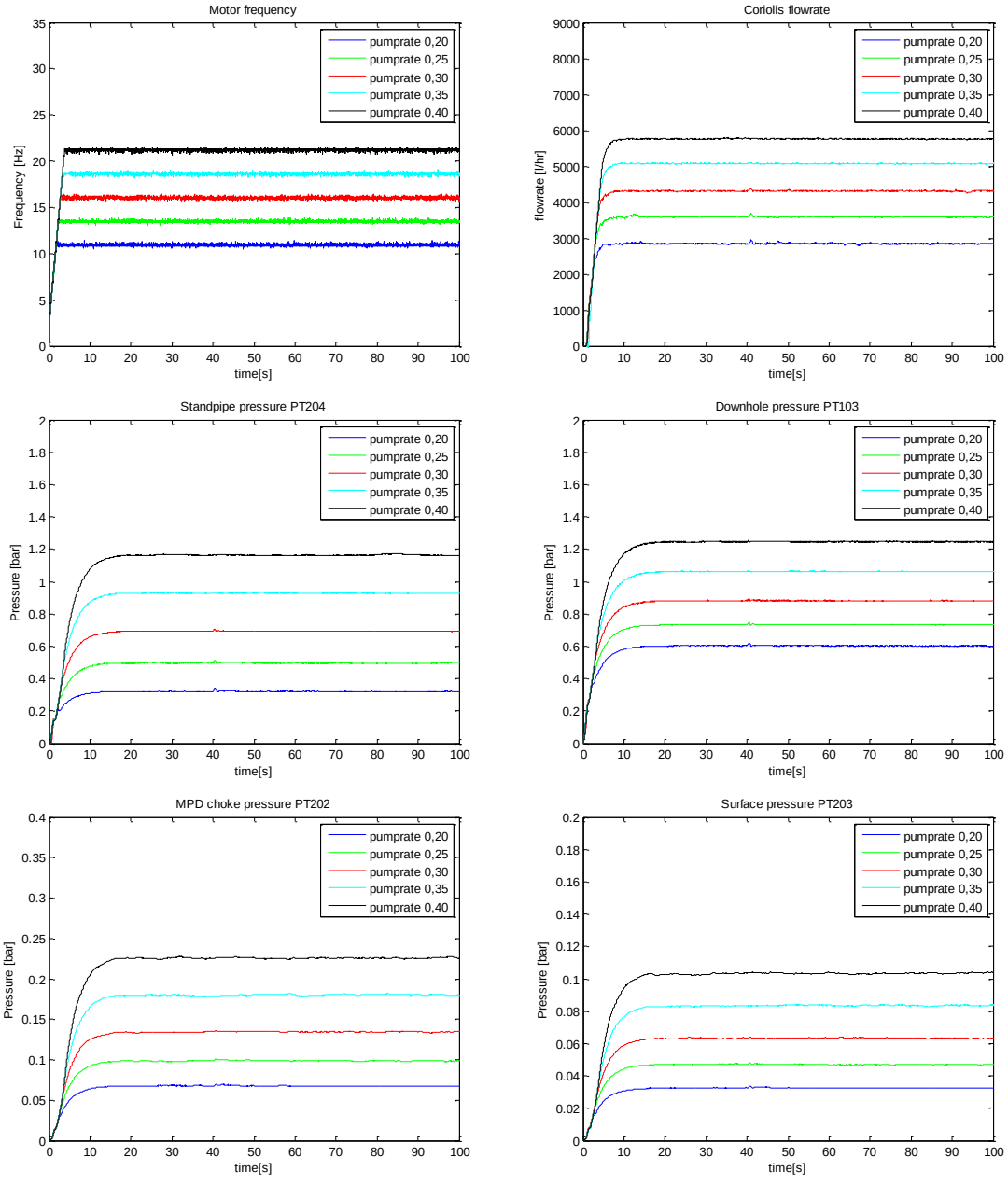

9) Experimental data for different pumprates with MPD choke open and influx 0,3 seconds with air pressure 2 bar.

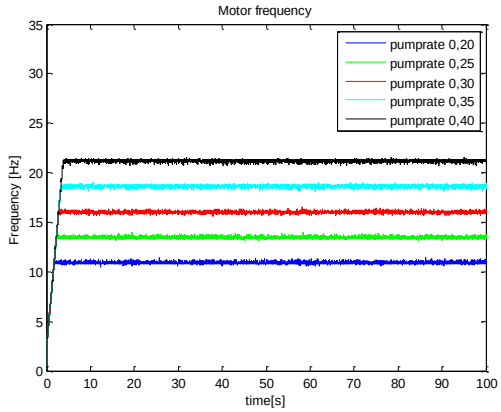

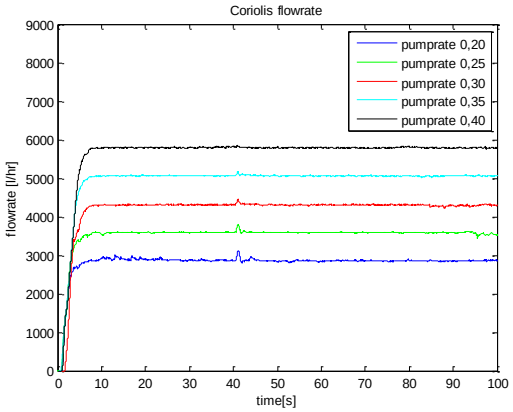

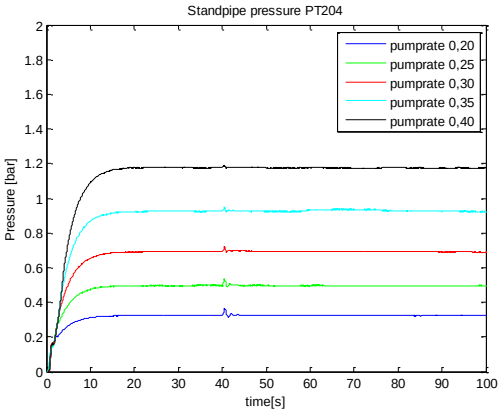

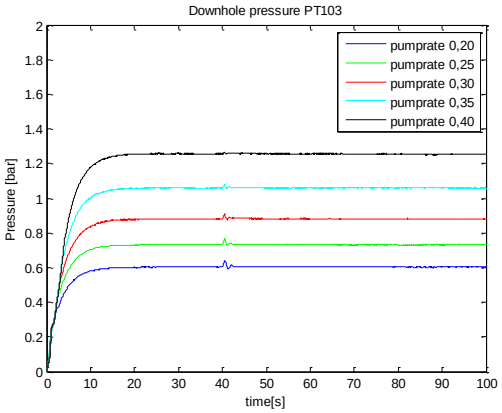

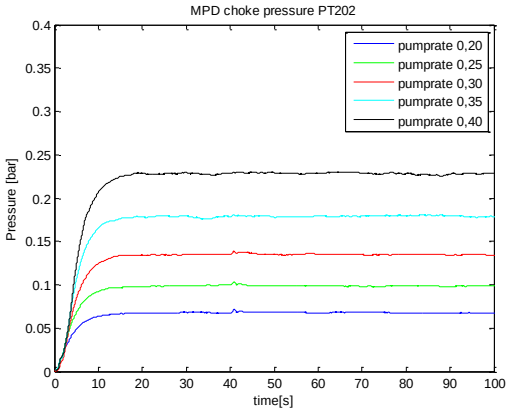

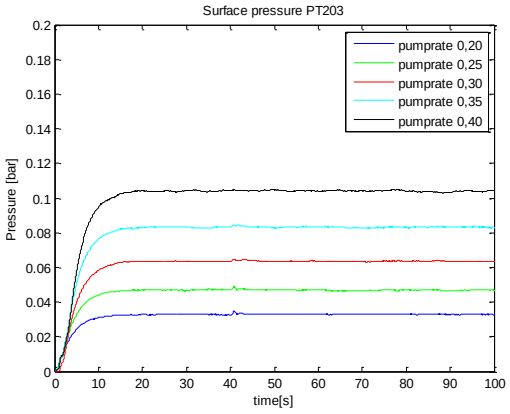

10) Experimental data for different pumprates with MPD choke open and influx 0,4 seconds with air pressure 2 bar.

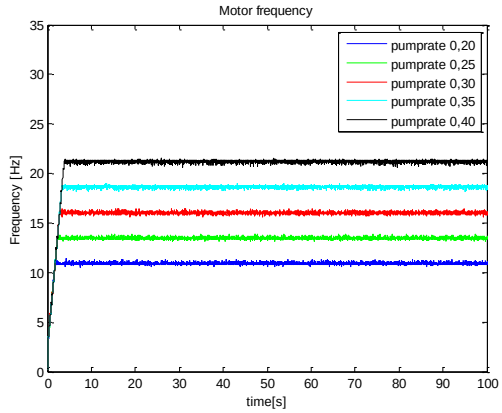

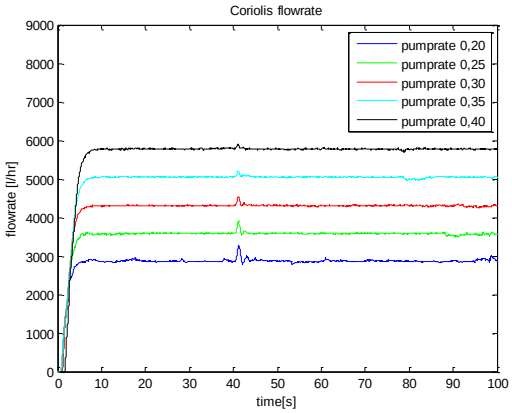

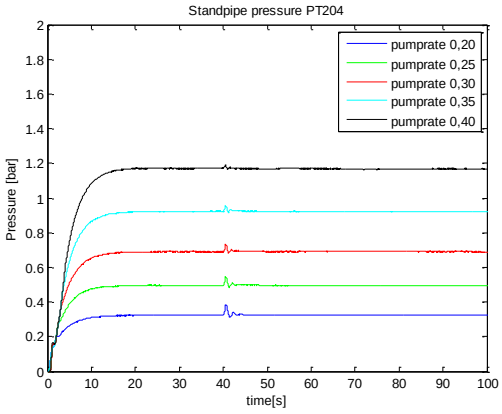

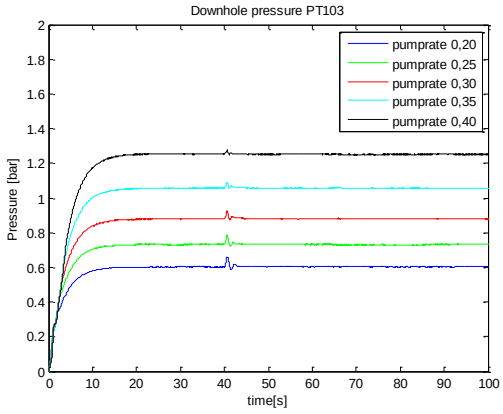

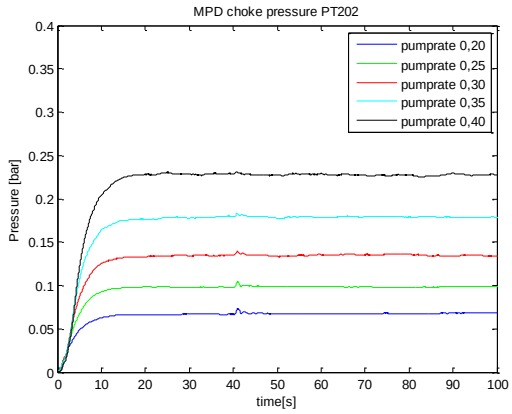

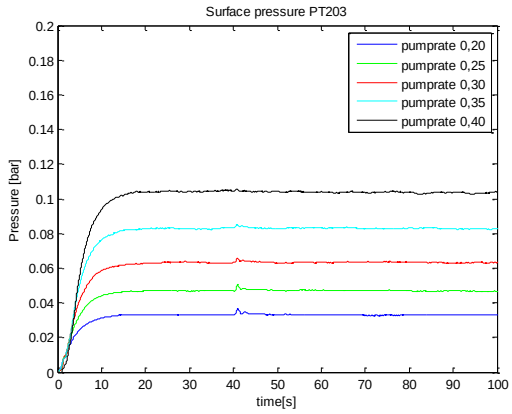

11) Experimental data for different pumprates with MPD choke open and influx 0,5 seconds with air pressure 2 bar.

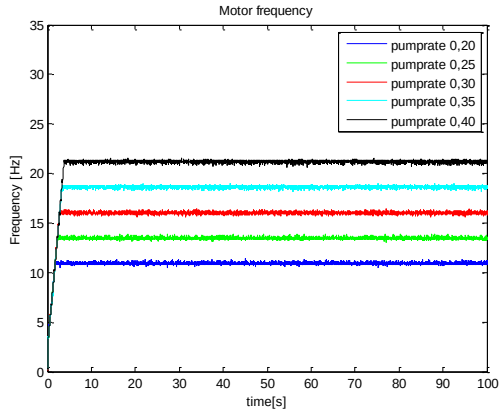

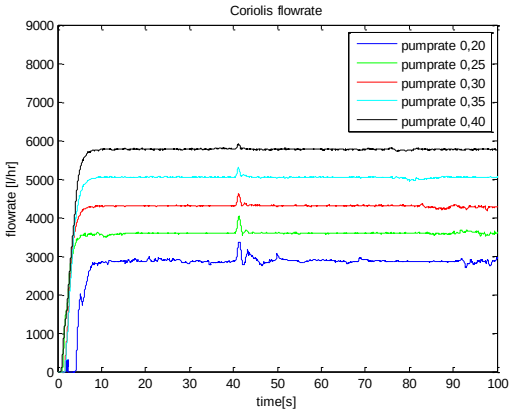

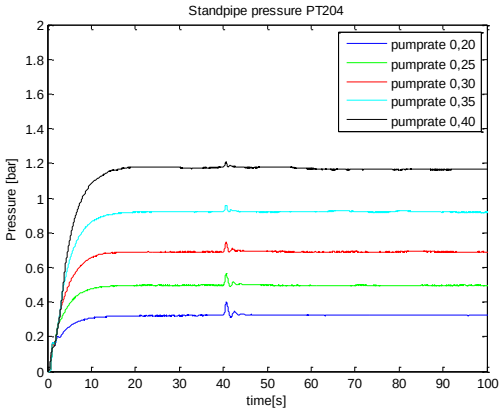

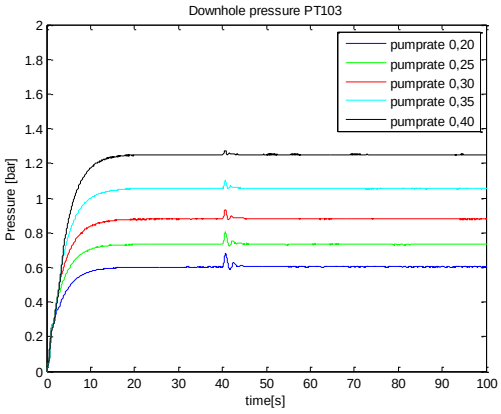

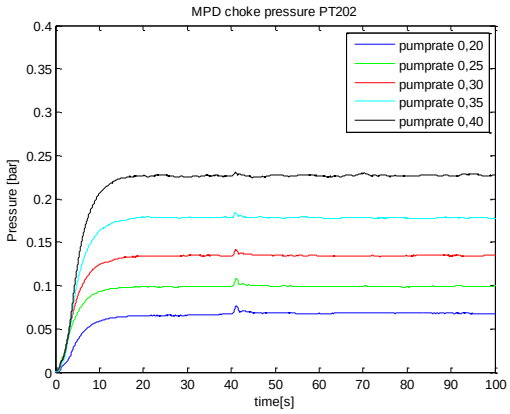

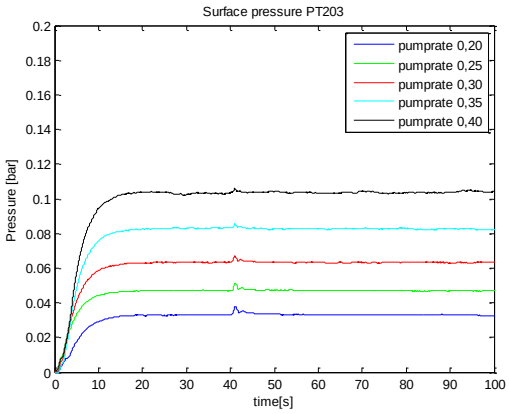

12) Experimental data for different pumprates with MPD choke open and influx 0,6 seconds with air pressure 2 bar.

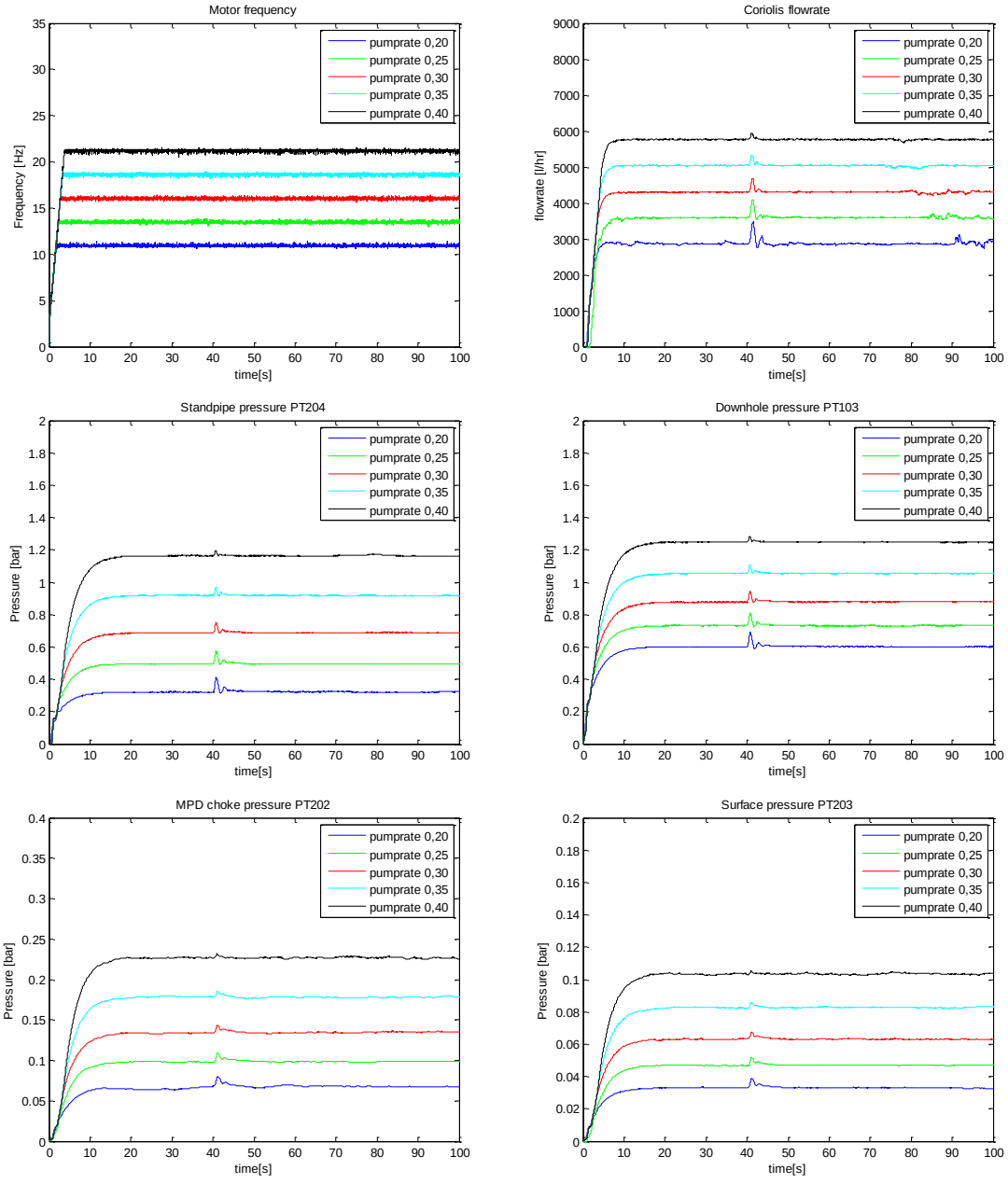

If take a closer look at the coriolis for influx time 0,6 s:

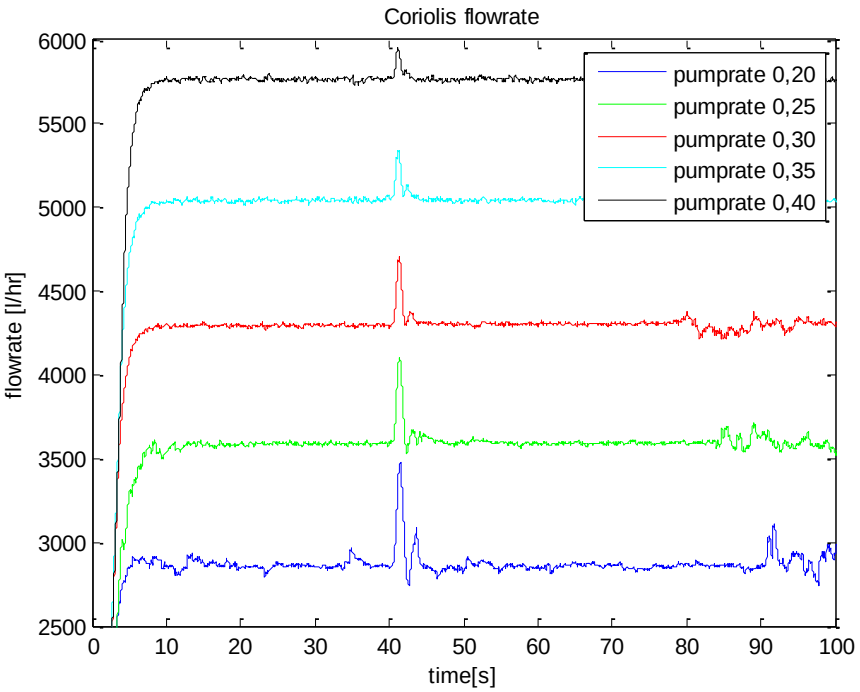

Comparison of the relative increase in flowrate for the different pumprates at influx:

- Pumprate 0,20: 21%
- Pumprate 0,25: 11%
- Pumprate 0,30: 9%
- Pumprate 0,35: 6%
- Pumprate 0,40: 3%

13) MPD choke opening set to 0,507 to obtain a 0,3 bar pressure margin with pumprate 0,25.

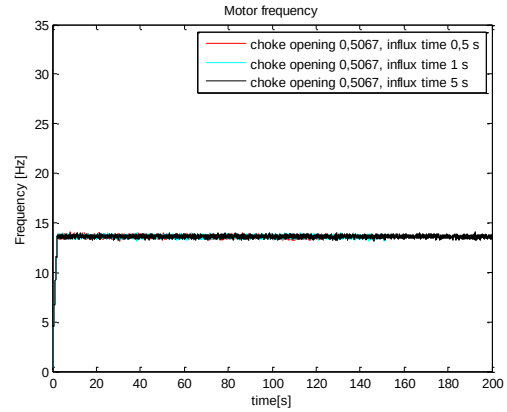

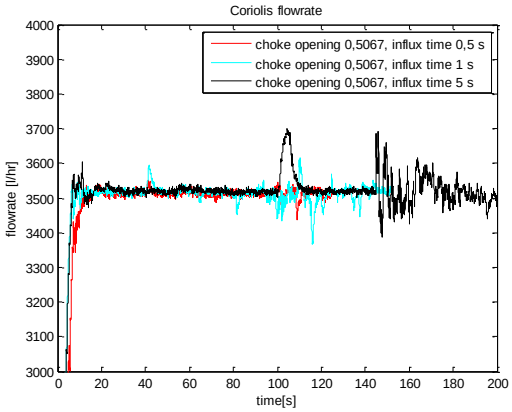

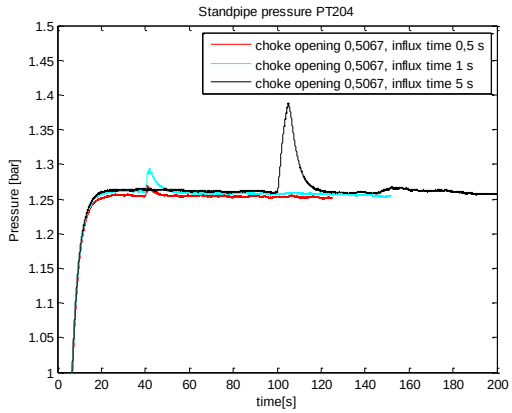

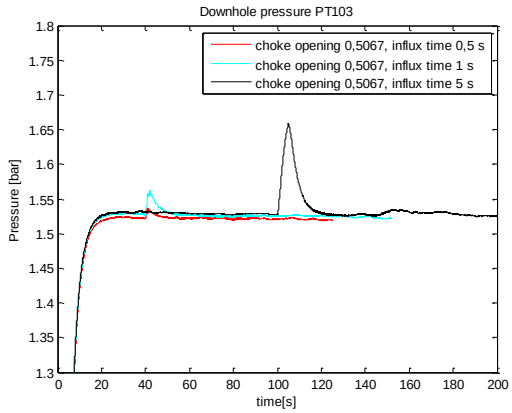

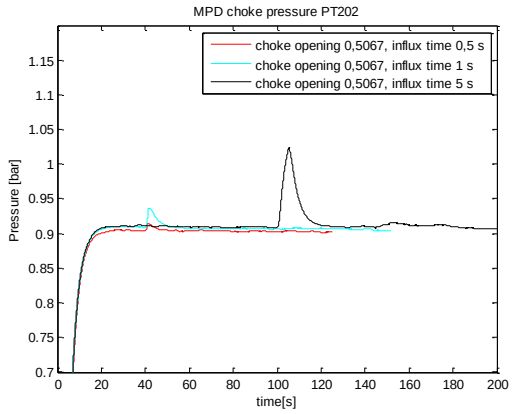

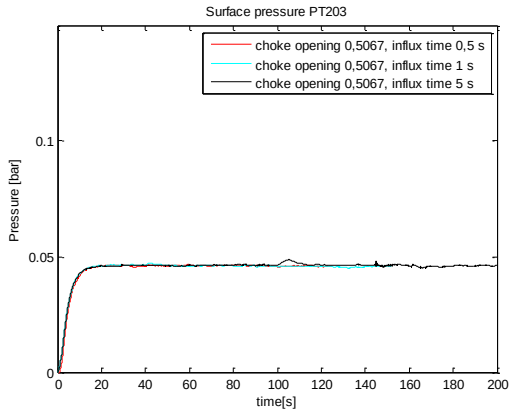

14) MPD choke opening set to 0,485 to obtain a 0,1 bar pressure margin with pumprate 0,25.

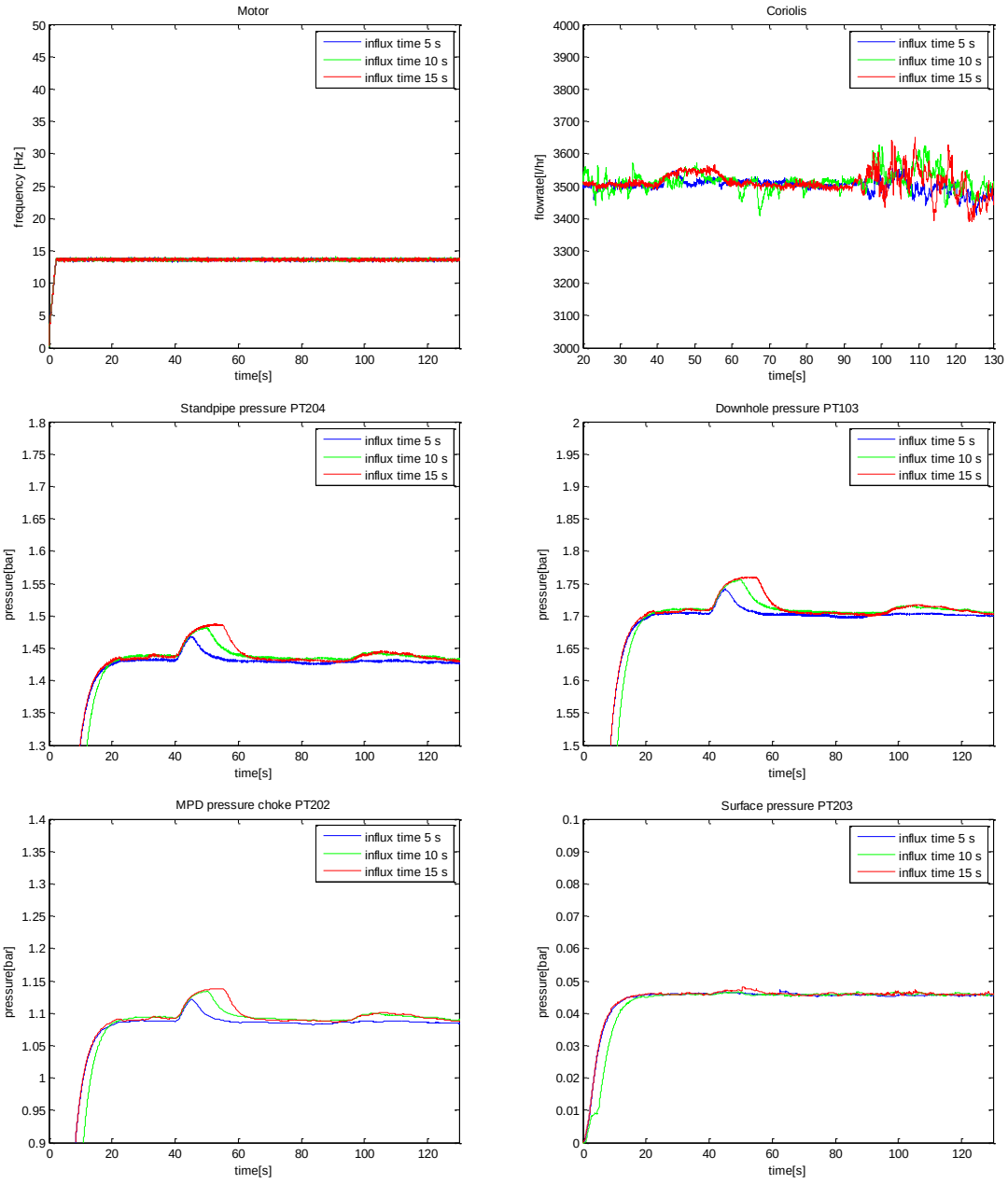

15) MPD choke opening set to 0,73 to obtain a 0,1 bar pressure margin with pumprate 0,40.

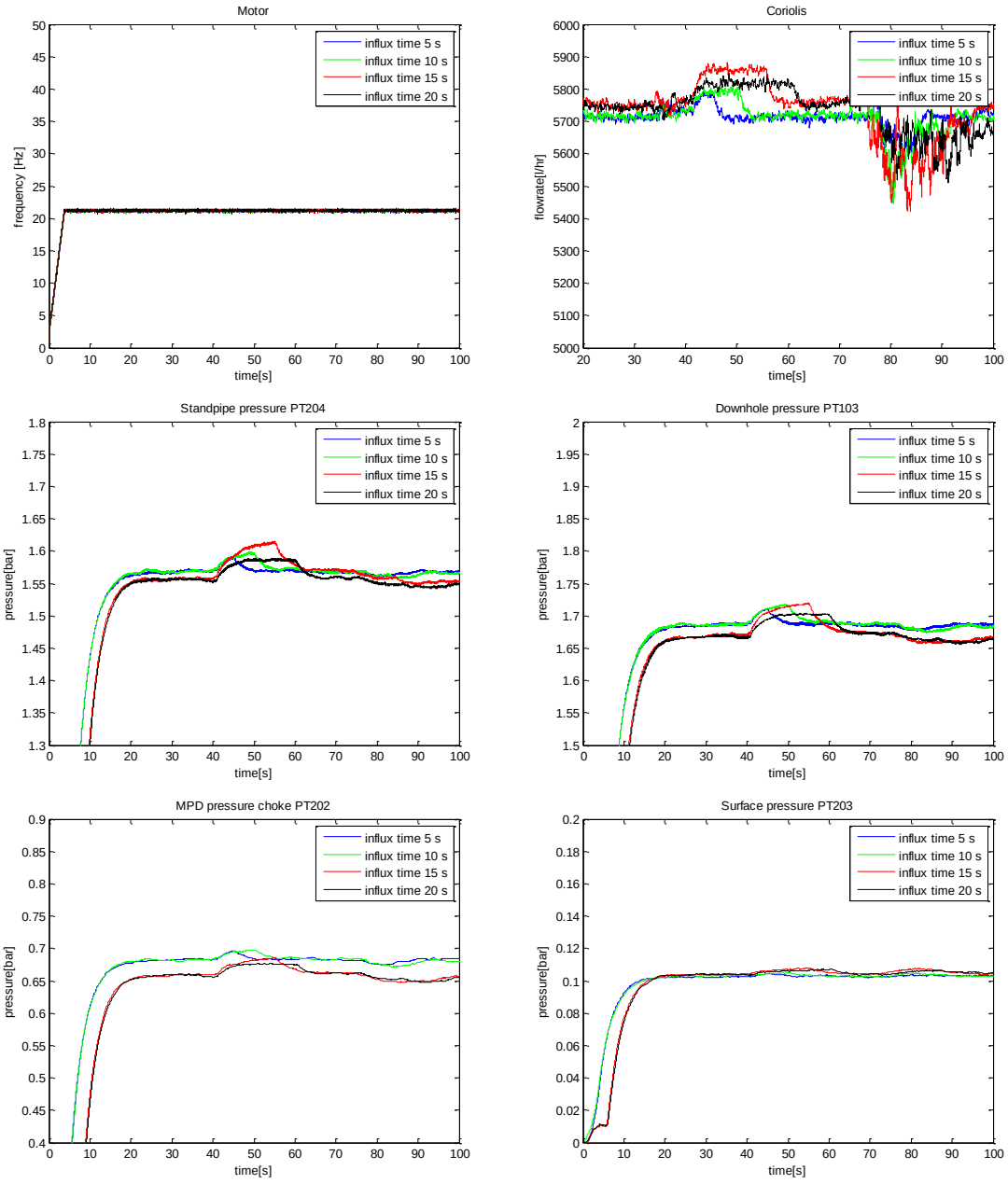

16) Loss with different pumprates from upper loss valve. MPD choke opening set to 0,73.

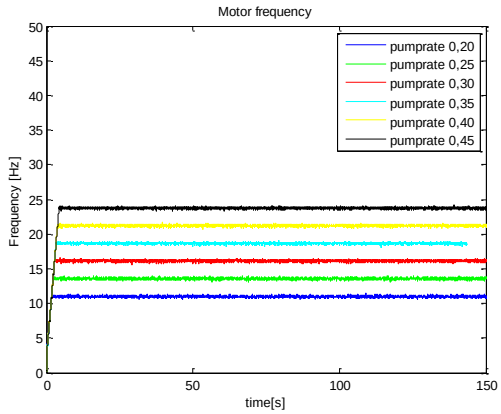

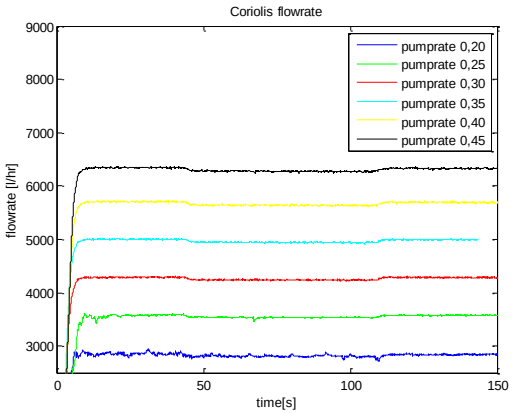

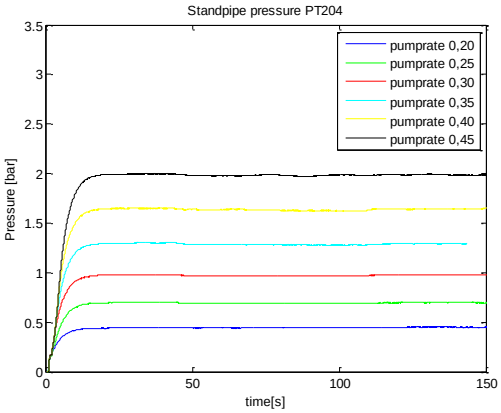

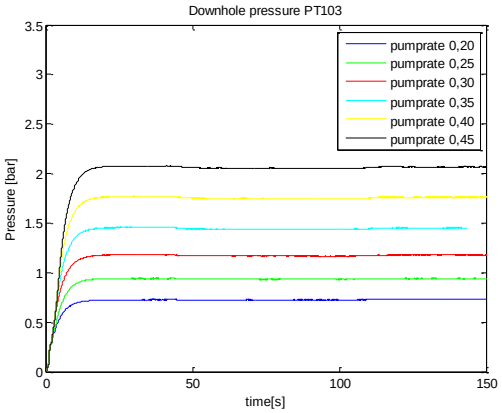

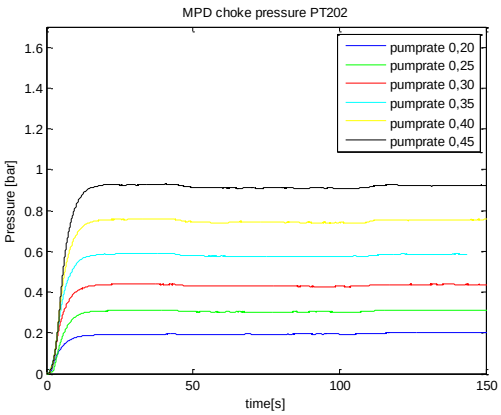

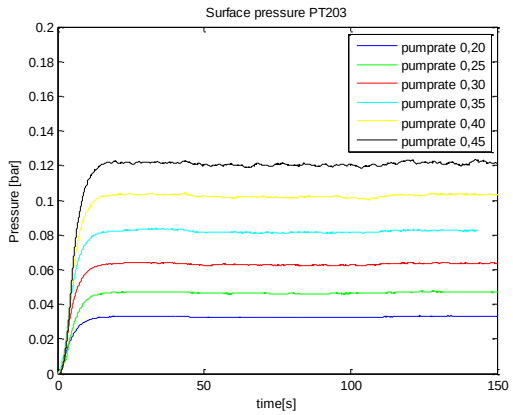

17) Loss with different pumprates from lower loss valve. MPD choke opening set to 0,73.

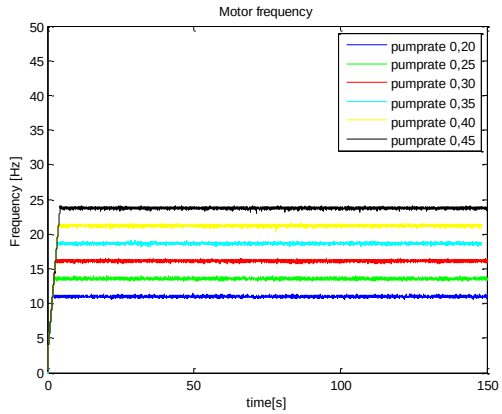

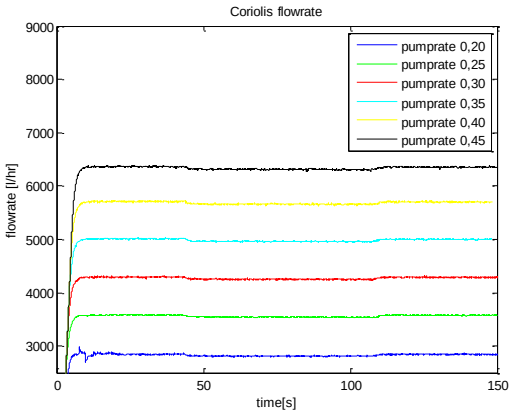

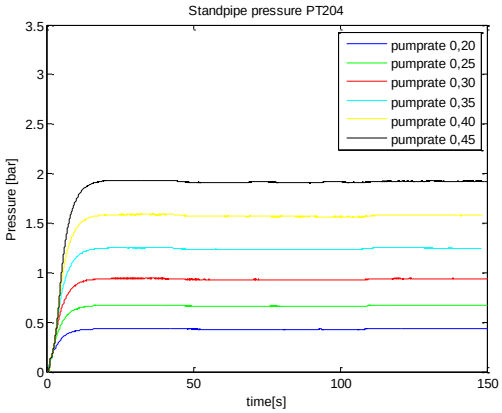

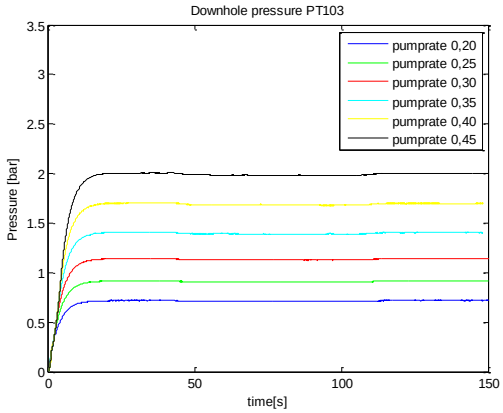

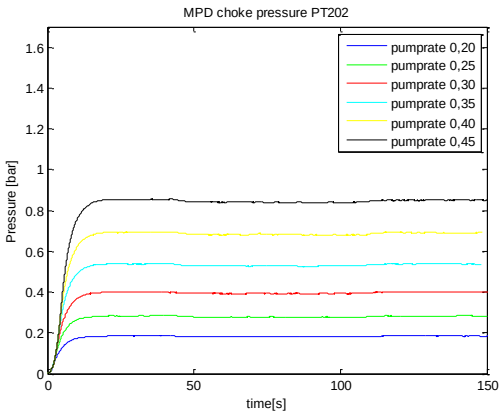

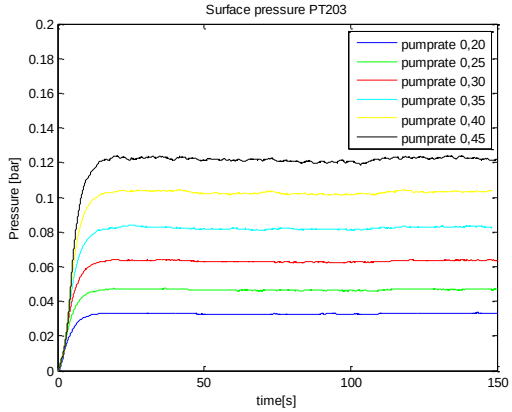

18) Loss with pumprate 0,25 and MPD choke opening set to 0,485.

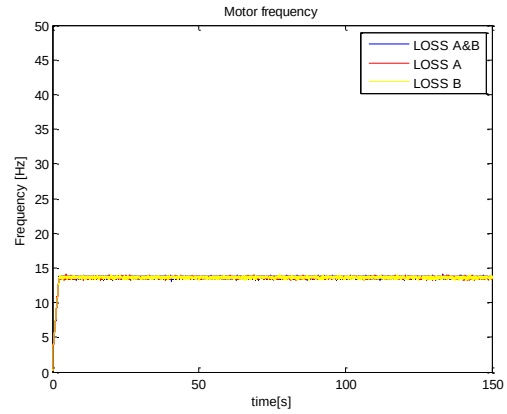

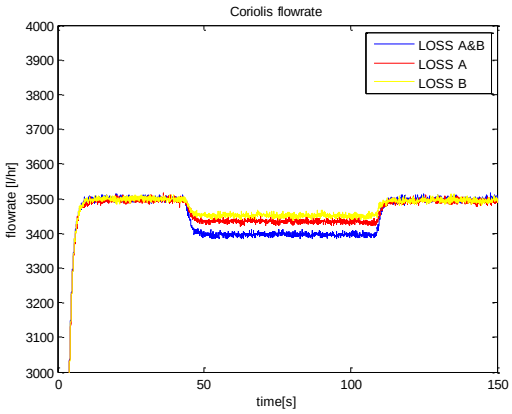

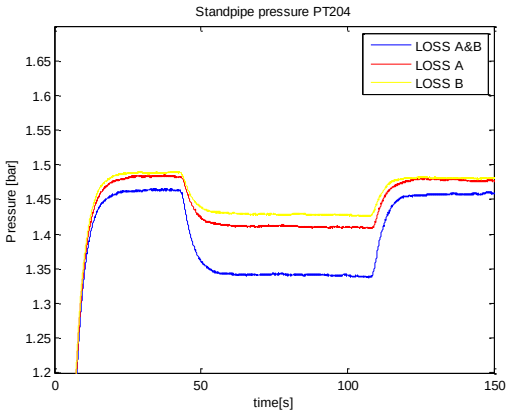

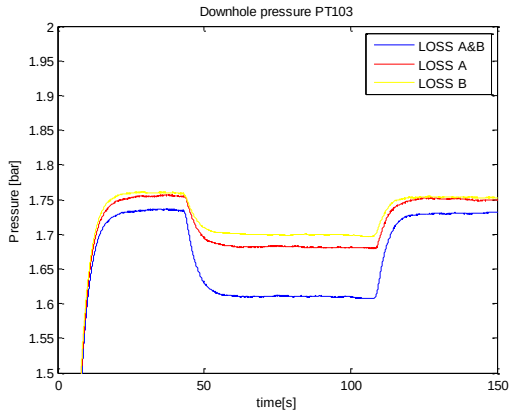

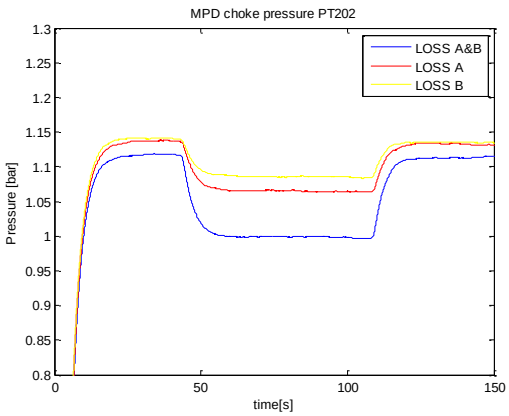

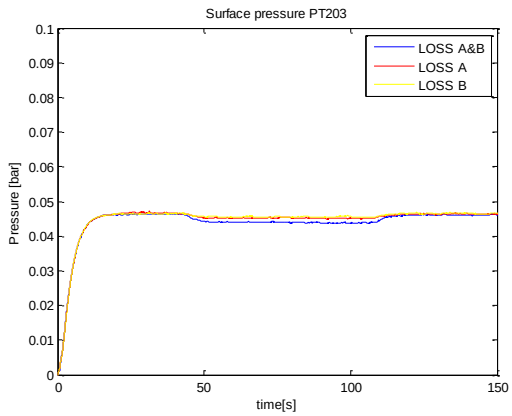

19) Loss with pumprate 0,25 and MPD choke opening set to 0,46.

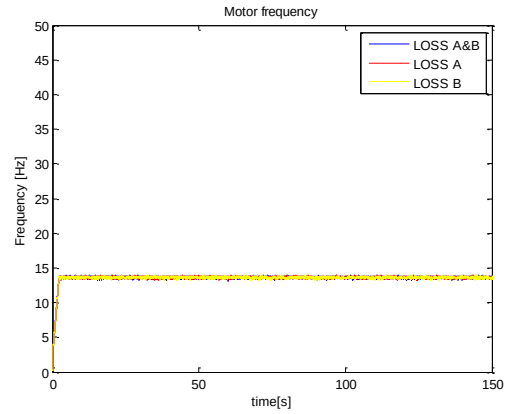

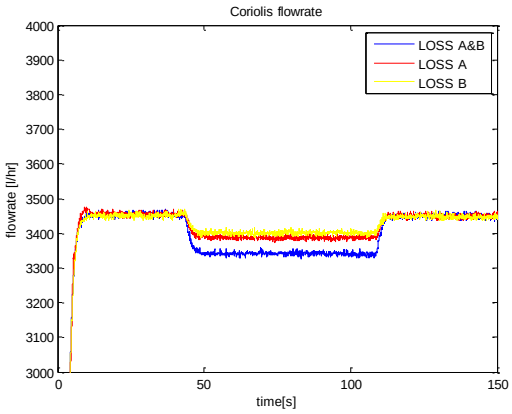

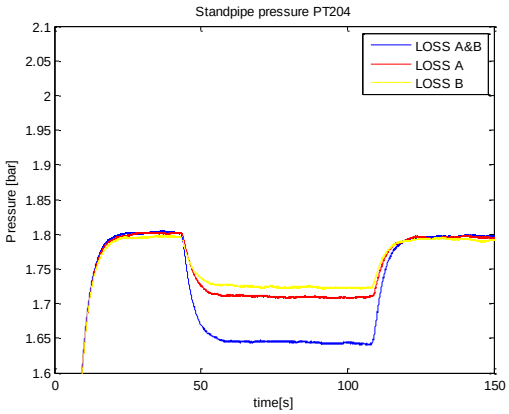

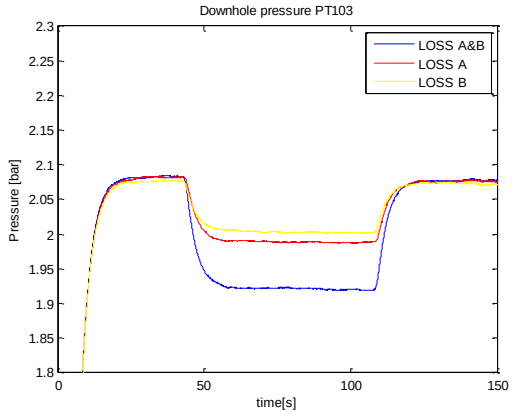

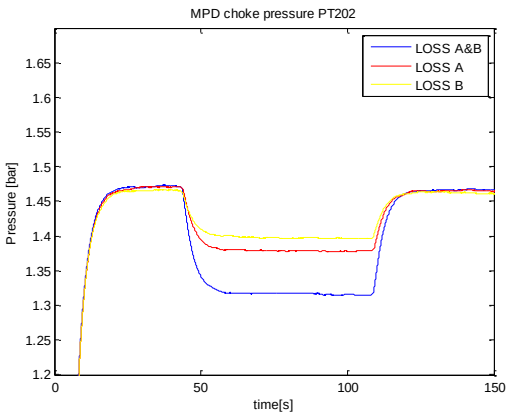

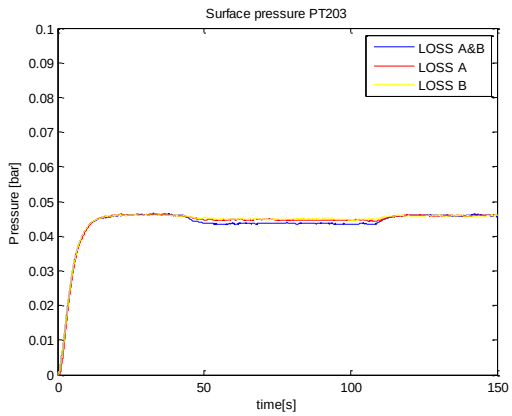

20) Loss with pumprate 0,40 and MPD choke opening set to 0,73.

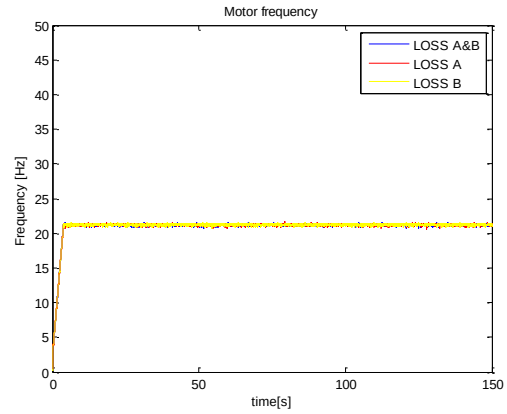

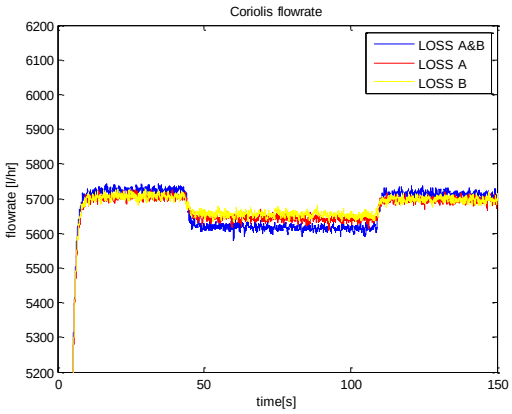

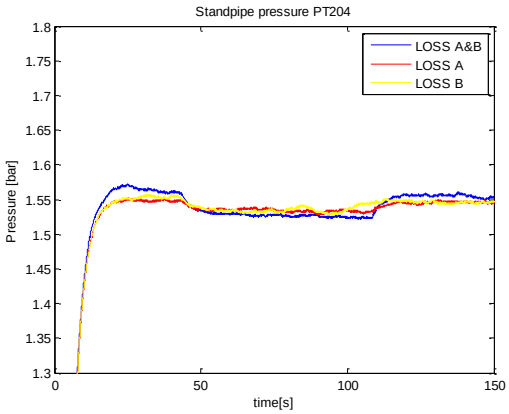

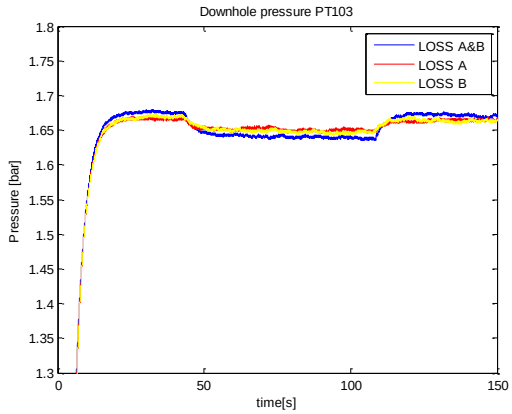

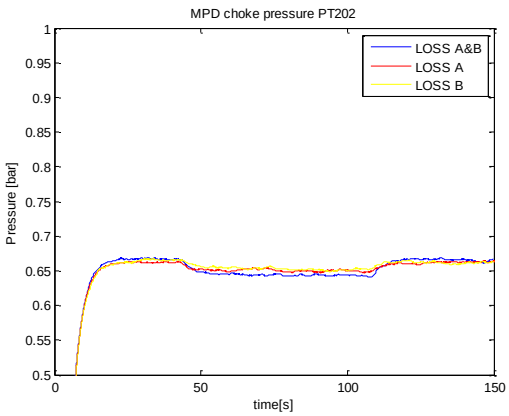

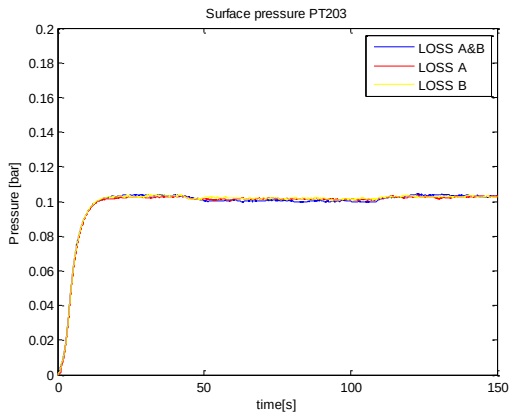

21) Loss with pumprate 0,40 and MPD choke opening set to 0,70.

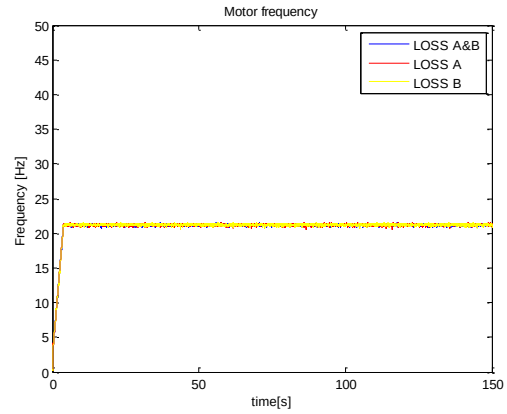

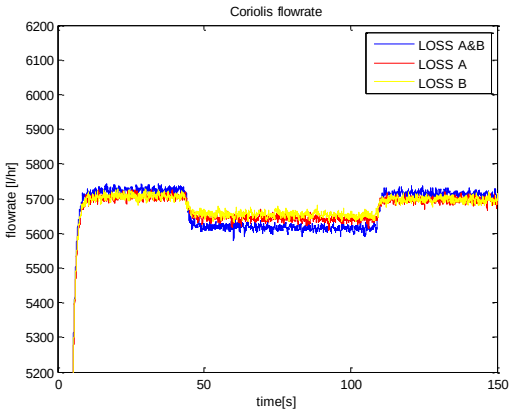

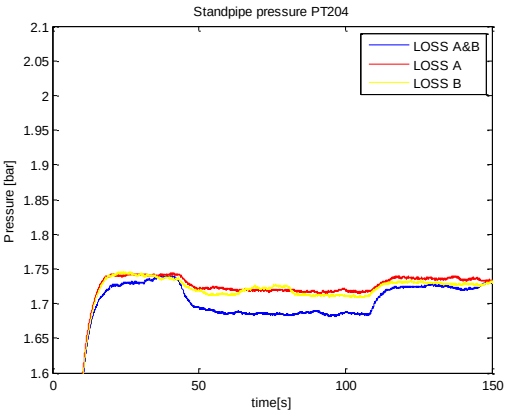

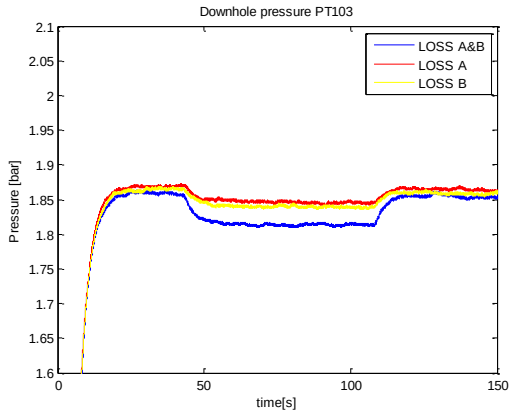

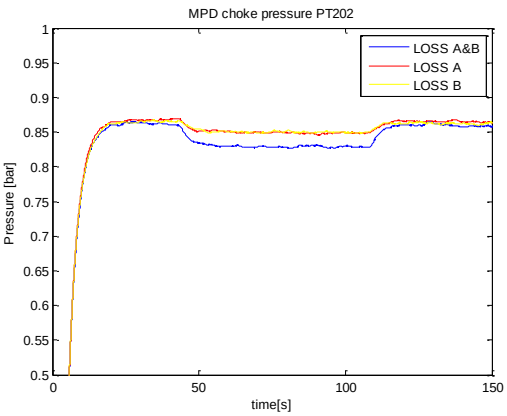

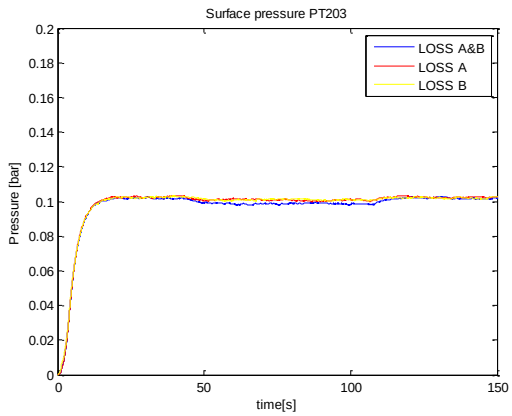

22) Different loss sizes from the upper loss valve with pumprate 0,30.

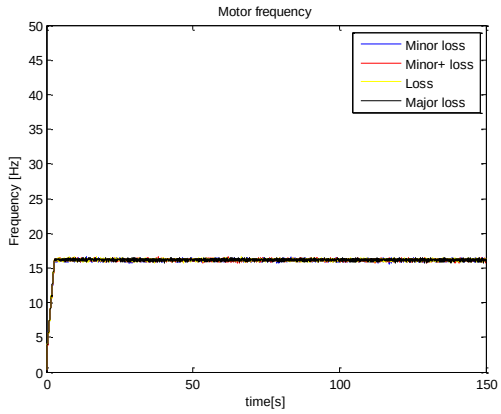

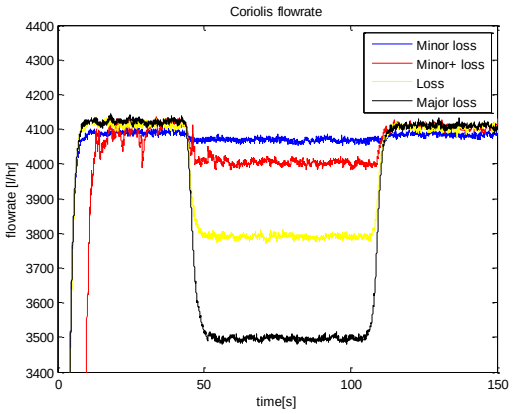

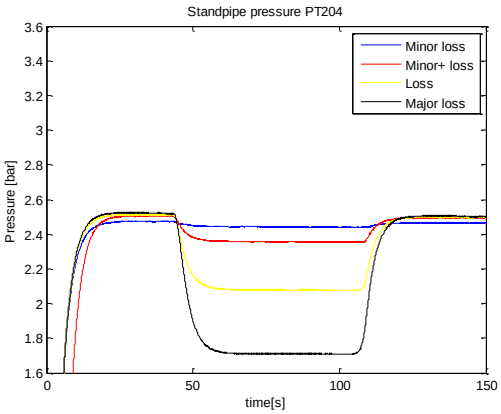

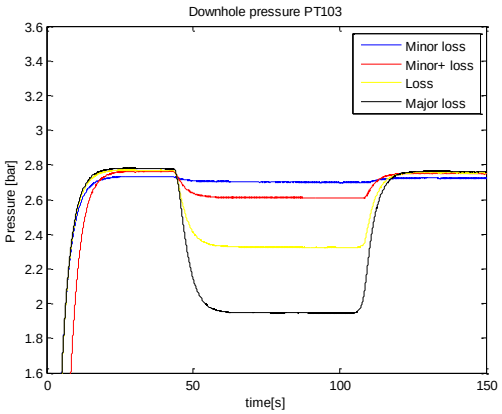

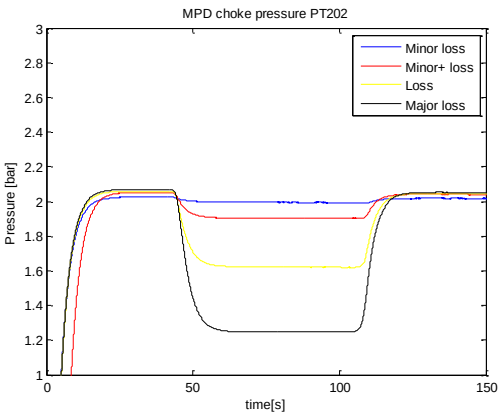

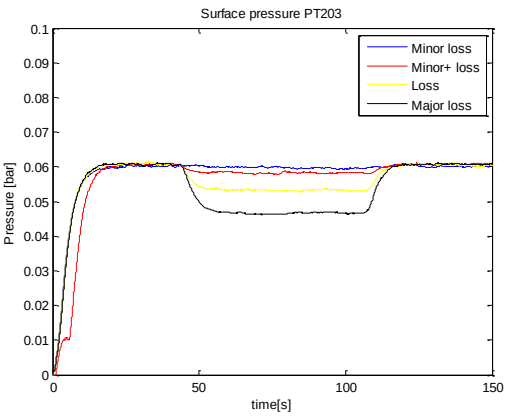

23) Different loss sizes from the lower loss valve with pumprate 0,30.

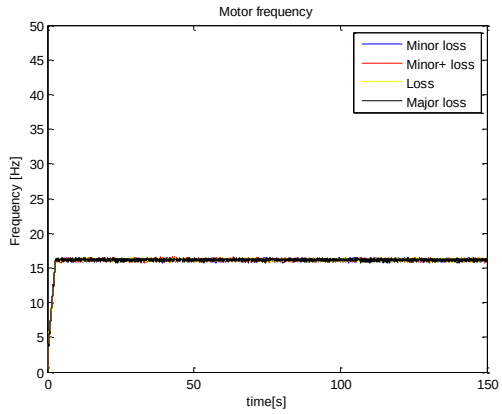

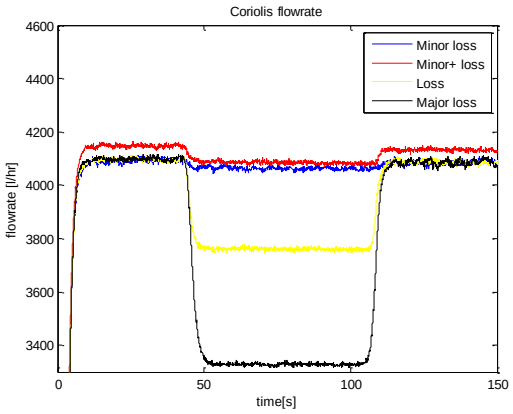

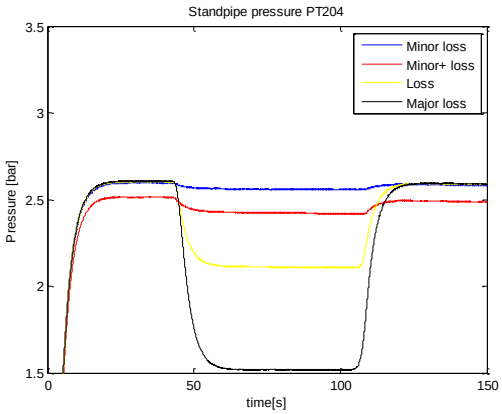

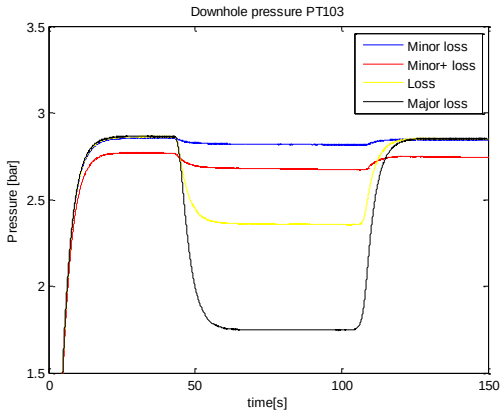

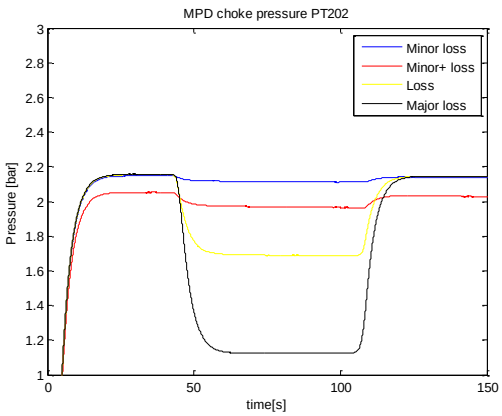

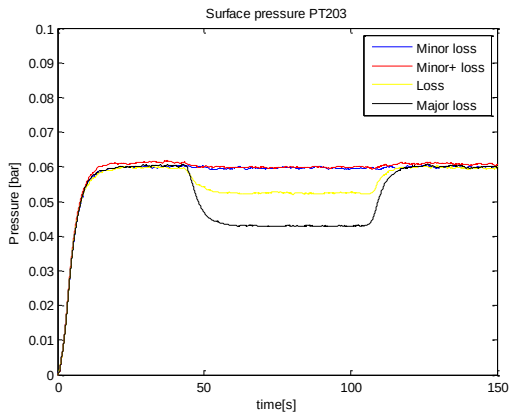

24) Loss from lower loss valve inducing kick.

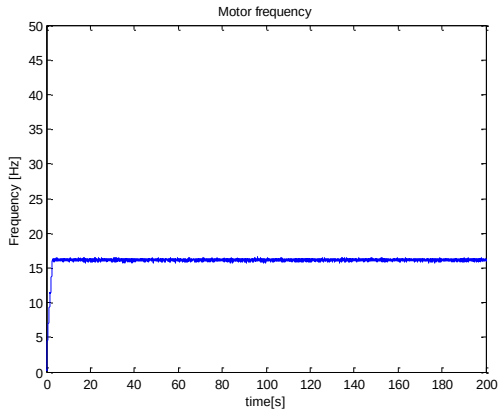

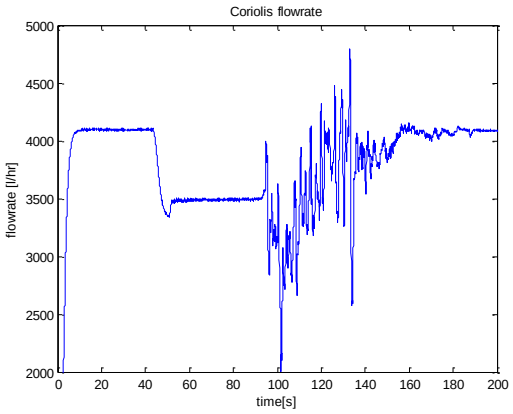

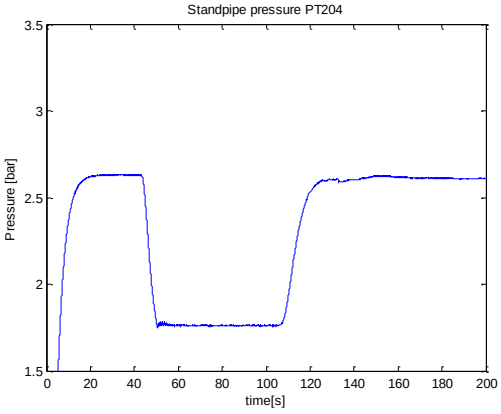

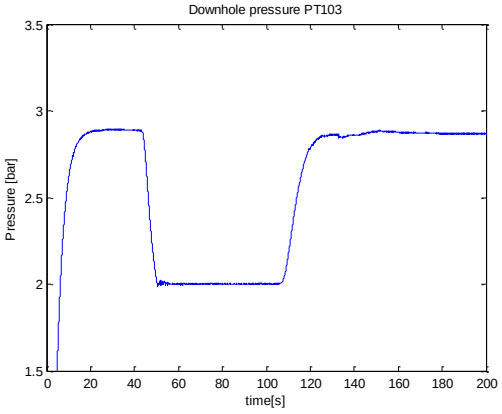

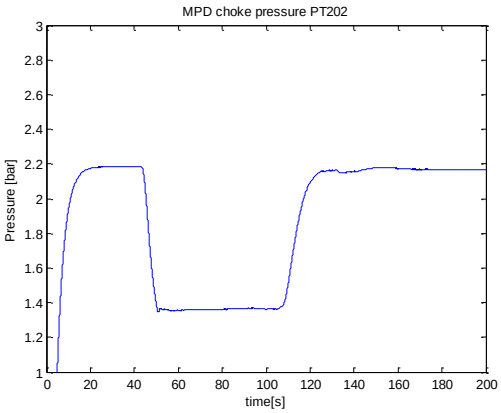

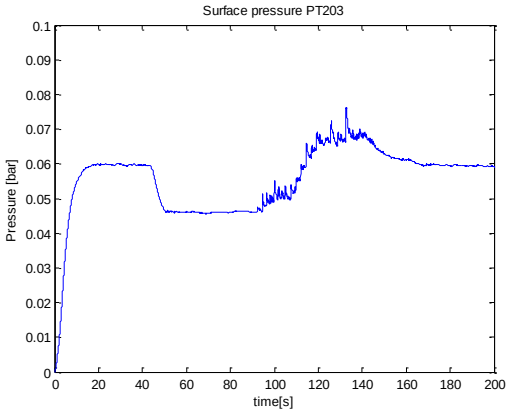

25) Loss from both loss valves inducing kick.

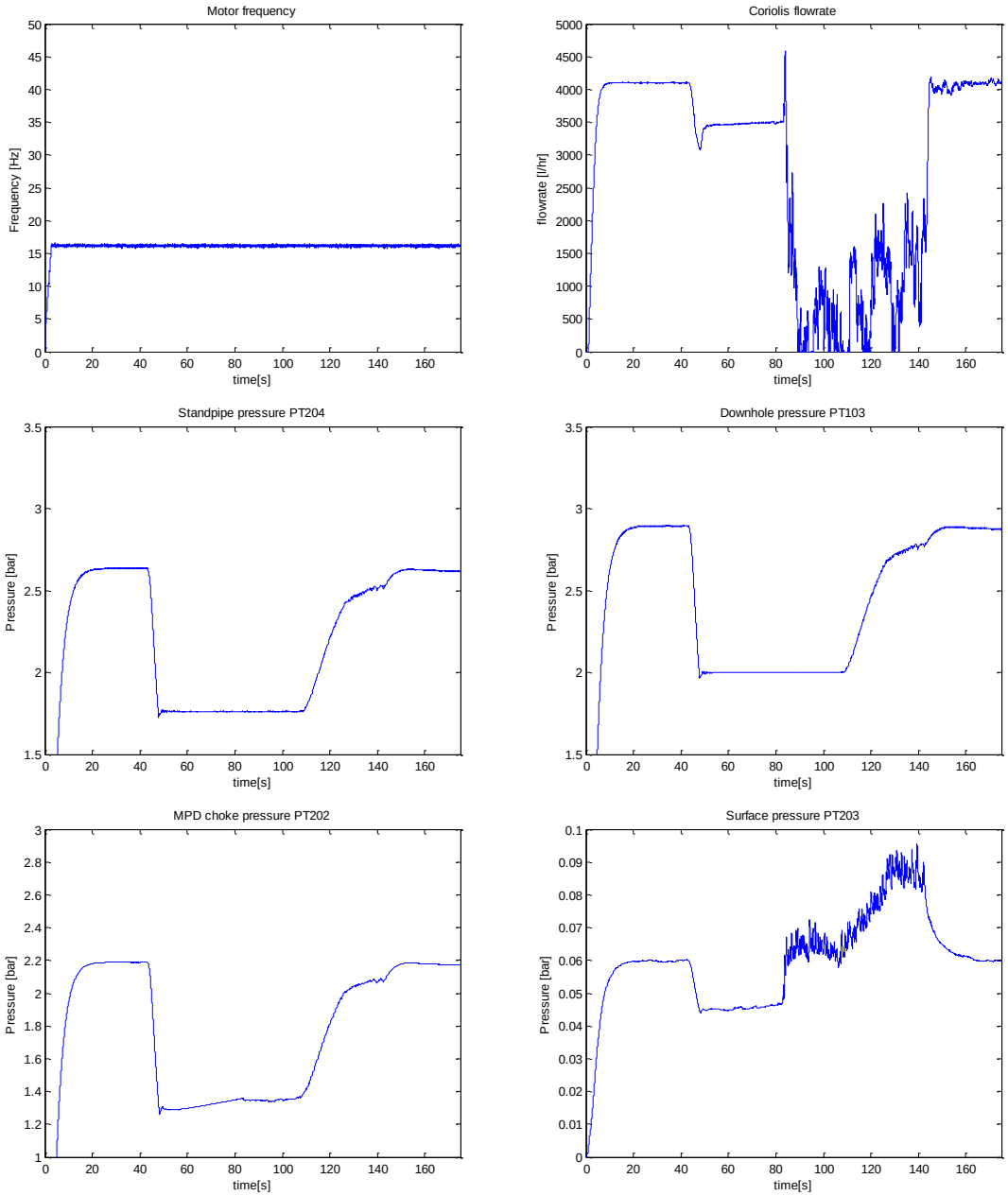

26) MPD automatic choke

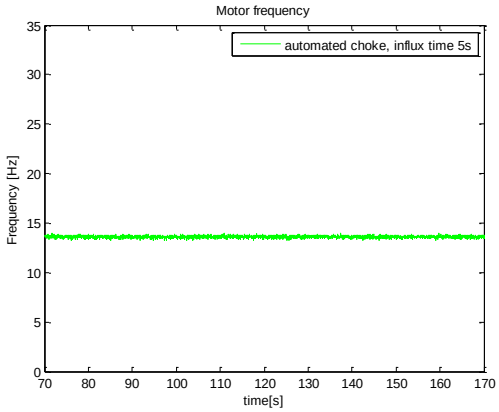

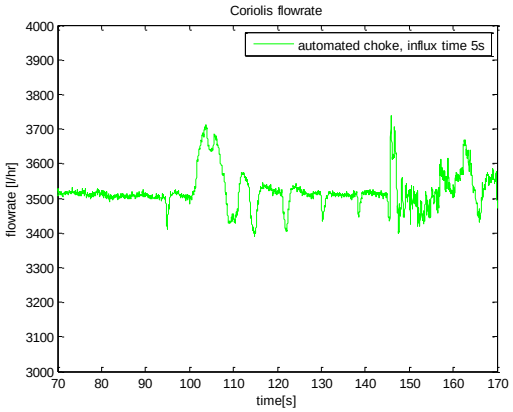

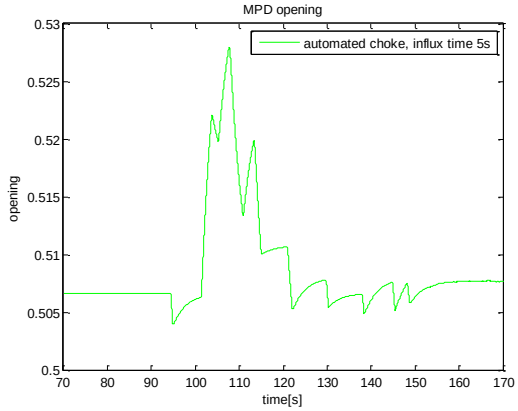

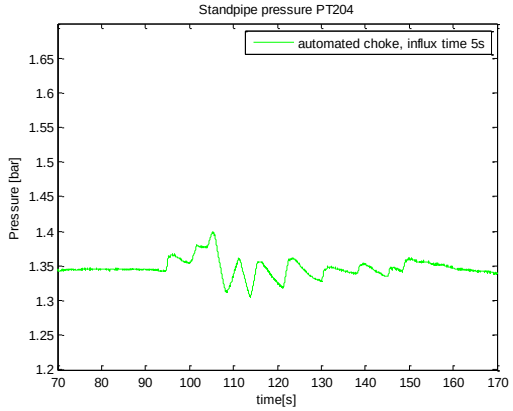

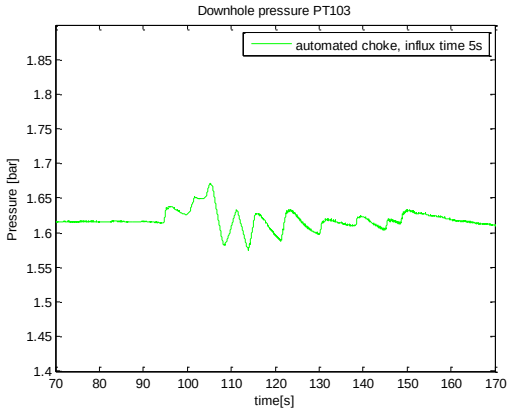

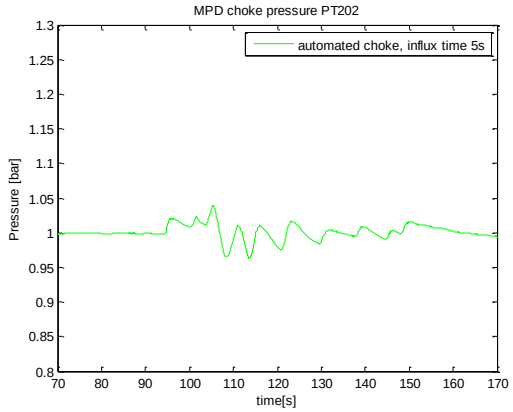

Appendix B

Test rig startup- and operational procedure

1) **Check water level in tank**. The water tank should be almost full when the rig is completely drained. The tank must never be less than 50% full when the rig system is filled with water. If this happens, the pump will suck air at high pumprates. Refill the tank when the rig is drained with clean water.

2) **Make sure all manual valves are in correct position before attempting to start the pump. Failure to do so can cause damage to the rig.** The correct starting positions of the valves are given in the figures on next page.

3) **Turn on the fan pointing towards the pump motor before starting the pump.** This is especially important at low pumprates (low motor frequency) to prevent the protective motor switch from breaking the circuit.

4) **Run Matlab code and Simulink model.**

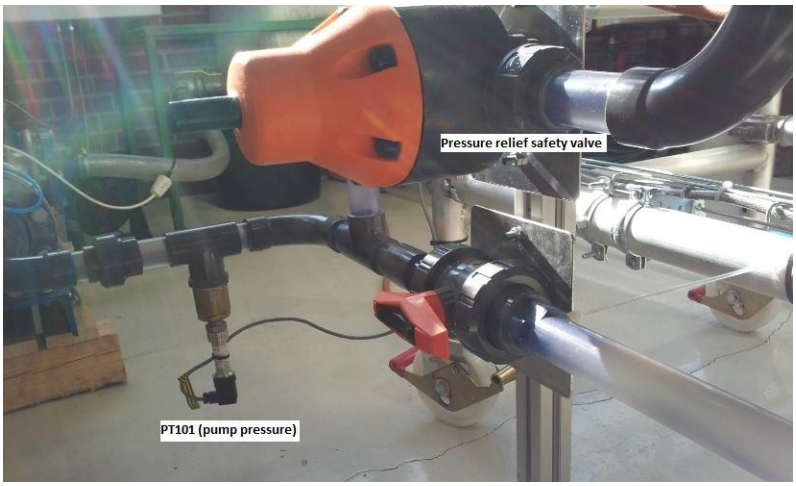

Water tank valve open. **Rig pipeline valve open.**

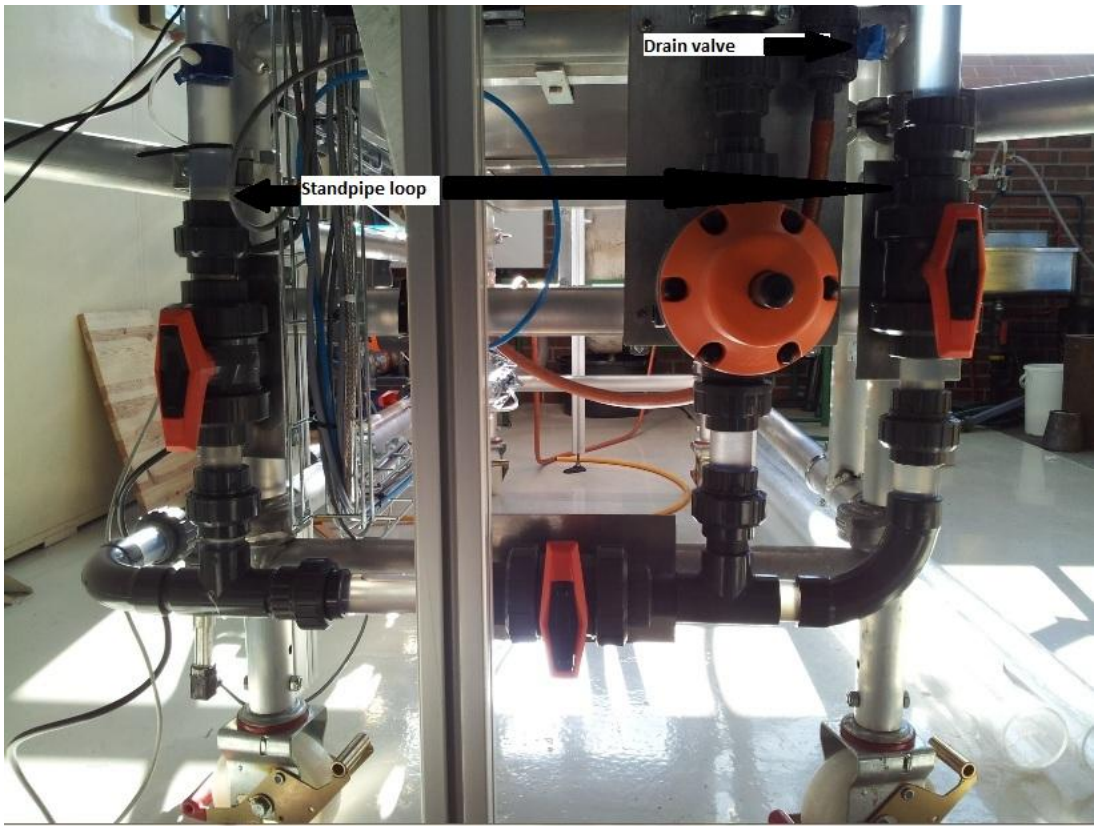

Standpipe routing chosen by opening standpipe loop valves and closing bottom valve. Drain valve closed.

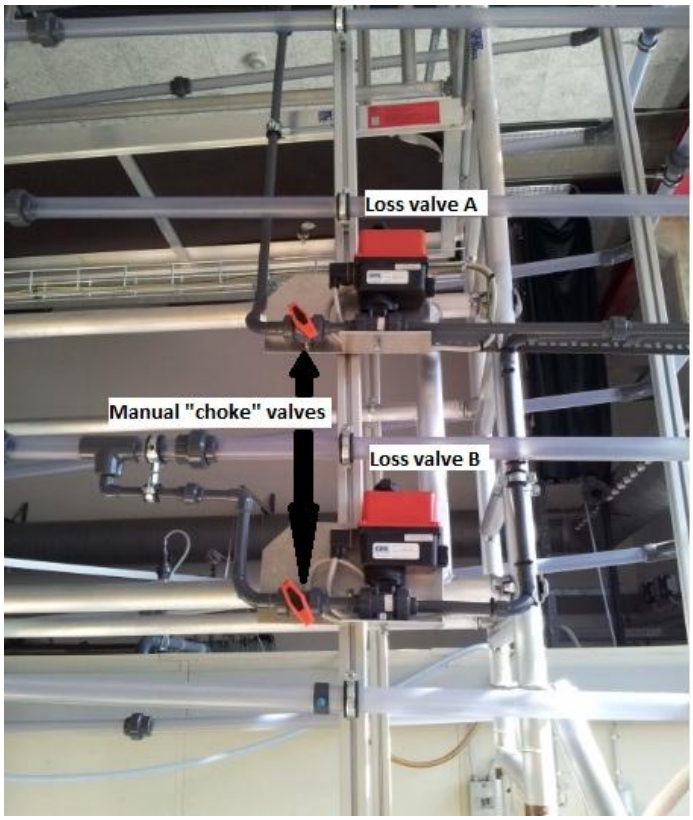

Automatic loss valves in closed position. Manual “choke” valves adjusted to allow desired efflux cross section.

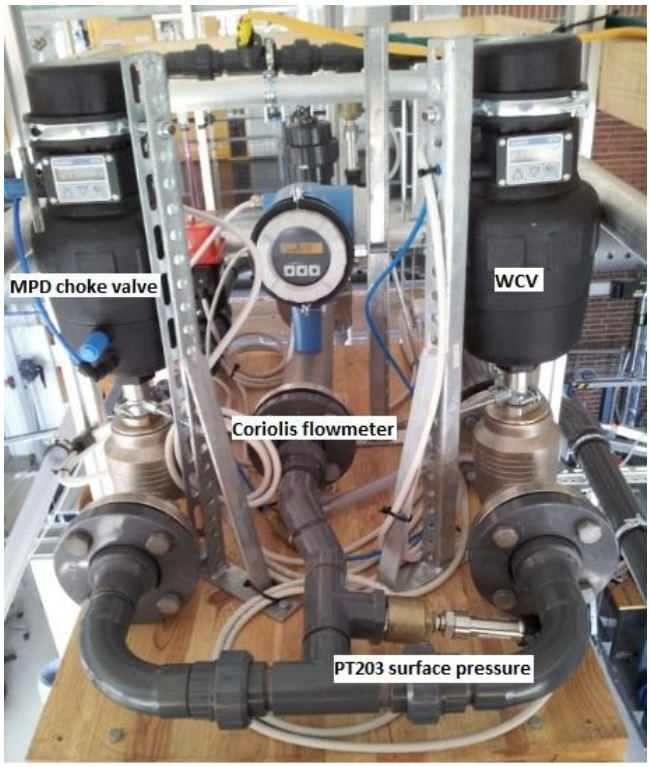

MPD choke valve, Well control valve, Coriolis flowmeter, Surface pressure transmitter.

Appendix C

Matlab calculations and scripts

Frictional pressure drop in test rig

■

```
clear all;
close all;

% calculated frictional pressure drop

rho = 1000;              % [kg/m^3]
A = pi*(0.0332/2)^2;     % [m^2]
my = 10^-3;              % [Pa*s]
D = 0.0332;              % [m]

pumprate1 = [0.20 0.25 0.30 0.35 0.40 0.45]; % fraction
coriolis = [2850 3590 4300 5040 5770 6460];  % [l/hr]

pumprate = pumprate1*50;     % [Hz]

q = coriolis/3600000;        % [ m^3/s]
u = q/A;                     % [m/s]
Re = rho*u*D/my;

f = 0.046*Re.^(-0.2);        % Dukler

% f = 0.0056+0.5*Re.^-(0.32) % Drew, Koo and McAdams

dpdx =(4/0.0332)*f.*0.5*rho.*u.^2;
dp = dpdx*57/10^5 % [bar]

polyfit(pumprate,dp,3);

new_P = 8:0.01:24;

P1 = polyval(polyfit(pumprate,dp,3),new_P);

figure;
plot(pumprate,dp,'rx',new_P,P1);
axis([5 25 0 0.9]);
title('Calculated frictional pressure drop');
xlabel('Pumprate [Hz]');
ylabel('dP friction [bar]');
saveas(gcf,'calculated pressure drop','meta');


% Using data registered by rig pressure transmitters to find
% frictional pressure drop

pt103 = [0.60 0.73 0.88 1.05 1.25 1.45];     % [bar]
pt202 = [0.07 0.10 0.13 0.18 0.23 0.28];     % [bar]
```

```
dp_friction = (pt103-pt202-0.4)              % [bar]

polyfit(pumprate,dp_friction,3);

P = polyval(polyfit(pumprate,dp_friction,3),new_P);

figure;
plot(pumprate,dp_friction,'o',new_P,P);
axis([5 25 0 0.9]);
title('Registered frictional pressure drop');
xlabel('Pumprate [Hz]');
ylabel('dP friction [bar]');
saveas(gcf,'pressure drop','meta');

% plot both in same graph
figure;
plot(pumprate,dp_friction,'g',new_P,P,pumprate,dp,'g',new_P,P1);
axis([5 30 0 1]);
title('Frictional pressure drop');
xlabel('Pumprate [Hz]');
ylabel('dP friction [bar]');
legend('calculated values','pressure transmitters');
saveas(gcf,'pressure drops','meta');
```

■

Example of plotscript:

17) Loss with different pumprates from lower loss valve. MPD choke opening set to 0,73.

■

```
close all;

load('LOSS_B_pumprate_0.20_loss_40-100s.mat');
pumprate_0_20=inngang;
load('LOSS_B_pumprate_0.25_loss_40-100s.mat');
pumprate_0_25=inngang;
load('LOSS_B_pumprate_0.30_loss_40-100s.mat');
pumprate_0_30=inngang;
load('LOSS_B_pumprate_0.35_loss_40-100s.mat');
pumprate_0_35=inngang;
load('LOSS_B_pumprate_0.40_loss_40-100s.mat');
pumprate_0_40=inngang;
load('LOSS_B_pumprate_0.45_loss_40-100s.mat');
pumprate_0_45=inngang;
```

```
% motor;
figure;
plot(pumprate_0_20.time,pumprate_0_20.signals(1).values,'b-
',pumprate_0_25.time,pumprate_0_25.signals(1).values,'g-
',pumprate_0_30.time,pumprate_0_30.signals(1).values,'r-
',pumprate_0_35.time,pumprate_0_35.signals(1).values,'c-
',pumprate_0_40.time,pumprate_0_40.signals(1).values,'y-
',pumprate_0_45.time,pumprate_0_45.signals(1).values,'k-');
axis([0 150 0 50]);
title('Motor frequency');
xlabel('time[s]');
ylabel('Frequency [Hz]');
legend('pumprate 0,20','pumprate 0,25','pumprate 0,30','pumprate
0,35','pumprate 0,40','pumprate 0,45');
saveas(gcf,'loss lower valve Motor','meta');
print Motor;

% standpipe pressure PT204;
figure;
plot(pumprate_0_20.time,pumprate_0_20.signals(8).values,'b-
',pumprate_0_25.time,pumprate_0_25.signals(8).values,'g-
',pumprate_0_30.time,pumprate_0_30.signals(8).values,'r-
',pumprate_0_35.time,pumprate_0_35.signals(8).values,'c-
',pumprate_0_40.time,pumprate_0_40.signals(8).values,'y-
',pumprate_0_45.time,pumprate_0_45.signals(8).values,'k-');
axis([0 150 0 3.5]);
title('Standpipe pressure PT204');
xlabel('time[s]');
ylabel('Pressure [bar]');
legend('pumprate 0,20','pumprate 0,25','pumprate 0,30','pumprate
0,35','pumprate 0,40','pumprate 0,45');
saveas(gcf,'loss lower valve PT204','meta');
print Standpipe_pressure;

% downhole pressure PT103;
figure;
plot(pumprate_0_20.time,pumprate_0_20.signals(4).values,'b-
',pumprate_0_25.time,pumprate_0_25.signals(4).values,'g-
',pumprate_0_30.time,pumprate_0_30.signals(4).values,'r-
',pumprate_0_35.time,pumprate_0_35.signals(4).values,'c-
',pumprate_0_40.time,pumprate_0_40.signals(4).values,'y-
',pumprate_0_45.time,pumprate_0_45.signals(4).values,'k-');
axis([0 150 0 3.5]);
title('Downhole pressure PT103');
xlabel('time[s]');
ylabel('Pressure [bar]');
legend('pumprate 0,20','pumprate 0,25','pumprate 0,30','pumprate
0,35','pumprate 0,40','pumprate 0,45');
saveas(gcf,'loss lower valve PT103','meta');
print Downhole_pressure;

% MPD choke PT202;
figure;
plot(pumprate_0_20.time,pumprate_0_20.signals(6).values,'b-
',pumprate_0_25.time,pumprate_0_25.signals(6).values,'g-
',pumprate_0_30.time,pumprate_0_30.signals(6).values,'r-
',pumprate_0_35.time,pumprate_0_35.signals(6).values,'c-
',pumprate_0_40.time,pumprate_0_40.signals(6).values,'y-
',pumprate_0_45.time,pumprate_0_45.signals(6).values,'k-');
axis([0 150 0 1.7]);
title('MPD choke pressure PT202');
```

```
xlabel('time[s]');
ylabel('Pressure [bar]');
legend('pumprate 0,20','pumprate 0,25','pumprate 0,30','pumprate
0,35','pumprate 0,40','pumprate 0,45');
saveas(gcf,'loss lower valve PT202','meta');
print MPD_pressure;

% Surface pressure PT203;
figure;
plot(pumprate_0_20.time,pumprate_0_20.signals(7).values,'b-
',pumprate_0_25.time,pumprate_0_25.signals(7).values,'g-
',pumprate_0_30.time,pumprate_0_30.signals(7).values,'r-
',pumprate_0_35.time,pumprate_0_35.signals(7).values,'c-
',pumprate_0_40.time,pumprate_0_40.signals(7).values,'y-
',pumprate_0_45.time,pumprate_0_45.signals(7).values,'k-');
axis([0 150 0 0.2]);
title('Surface pressure PT203');
xlabel('time[s]');
ylabel('Pressure [bar]');
legend('pumprate 0,20','pumprate 0,25','pumprate 0,30','pumprate
0,35','pumprate 0,40','pumprate 0,45');
saveas(gcf,'loss lower valve PT203','meta');
print Surface_pressure;

% Coriolis flowrate;
figure;
plot(pumprate_0_20.time,pumprate_0_20.signals(11).values,'b-
',pumprate_0_25.time,pumprate_0_25.signals(11).values,'g-
',pumprate_0_30.time,pumprate_0_30.signals(11).values,'r-
',pumprate_0_35.time,pumprate_0_35.signals(11).values,'c-
',pumprate_0_40.time,pumprate_0_40.signals(11).values,'y-
',pumprate_0_45.time,pumprate_0_45.signals(11).values,'k-');
axis([0 150 2500 9000]);
title('Coriolis flowrate');
xlabel('time[s]');
ylabel('flowrate [l/hr]');
legend('pumprate 0,20','pumprate 0,25','pumprate 0,30','pumprate
0,35','pumprate 0,40','pumprate 0,45');
saveas(gcf,'loss lower valve Coriolis','meta');
print Coriolis_flowrate;
```

■